# Unraveling a Vicious Cycle: The Interplay Between Extreme Weather Events, Urban Expansion, and Deforestation

Leonie Ratzke* Melanie Krause† Sebastian Sippel‡

May 30, 2024

**Abstract**

We examine the nexus between extreme weather events, urban expansion and tree cover loss in a global data set of regions from 163 countries spanning the years 2001-2018. We delve into how droughts and floods may drive rural-urban migration, triggering urban expansion that often leads to deforestation. This deforestation can in turn exacerbate flood and drought damages. Employing a four-equation Simultaneous Equations Model, we provide evidence of a vicious cycle of tree cover loss, increased drought damages and urban expansion at the global scale. Yet, we also find substantial spatial heterogeneity, especially for the role of tree cover loss in attenuating or amplifying drought damages. We differentiate by world region and development level to show varying dynamics of urban expansion, deforestation and damages, with relevant policy implications for managing urban growth and environmental sustainability.

**JEL Classification:** Q54, Q23, O18, R11

**Keywords:** Natural Disasters, Urbanization, Deforestation, Feedback Loop, Simultaneous Equation Model

---

This paper has been presented at Fraunhofer Institute for Systems and Innovation Research ISI, Jena University as well as internal workshops at Leipzig University. We would like to thank Hannes Feilhauer, Miguel Mahecha and other seminar participants of the Breathing Nature excellence cluster initiative for helpful comments and suggestions. We gratefully acknowledge funding from the Saxon State Ministry for Science, Culture and Tourism (SMWK) – [3-7304/44/4-2023/8846].

*Leipzig University, Faculty of Economics and Management Sciences, Grimmaische Straße 12, 04109 Leipzig, Germany. E-mail: *leonie.ratzke@uni-leipzig.de*

†Leipzig University, Faculty of Economics and Management Sciences, Grimmaische Straße 12, 04109 Leipzig, Germany. E-mail: *melanie.krause@uni-leipzig.de*

‡Leipzig University, Faculty of Physics and Earth System Sciences, Talstraße 35, 04103 Leipzig, Germany. E-mail: *sebastian.sippel@uni-leipzig.de*

# 1 Introduction

Extreme climate and weather events, such as droughts and floods are occurring with increased frequency and intensity in times of climate change (Stocker, 2014, Zhang et al., 2013). Together with increasing human exposure (Ehrlich et al., 2018), we see a positive trend in resulting humanitarian disasters. However, it is not only increasing exposure, but also rapid urbanization as well as tree cover loss that may play a role here. In this paper, we study the interconnectedness between increased disaster impacts, urbanization, and tree cover loss with econometric methods.

The literature has typically focused on individual links between two of these three developments, respectively. For instance, floods and droughts have been shown to drive migration from rural to urban areas, propelling urbanization in developing countries (Cattaneo and Peri, 2016, Castells-Quintana et al., 2021, Kaczan and Orgill-Meyer, 2020). As cities expand, the trade-off in land use often leads to land-use change typically increasing sealed areas and decreasing tree cover (van Vliet, 2019, Huang et al., 2018, Behnisch et al., 2022). A loss in forest cover then can potentially increase flood damages due to reduced water retention potential and increase drought damages due to reduced soil water storage capacity (Bradshaw et al., 2007, Tembata et al., 2020, Haile et al., 2019). Cascading effects of this kind are yet under-researched in the empirical literature. It is the goal of our paper to study the importance of the interrelations between these three phenomena.

We construct a data set of variables at the regional level (NUTS-1) from around the world from 2001 to 2018. It contains 2079 regions in 163 countries that have experienced at least one drought or flood event impacting humans within that period. Our four main variables are change in urban size, deforestation, as well as flood- and drought related damages. In addition, we have a total of 13 control variables based on insights from the literature.

In contrast to previous studies, we do not consider each relation separately, but focus on the their interconnectedness in a whole vicious cycle. We do so by setting up a four-equation Simultaneous Equations Model (SEM) to capture the interdependencies of urban growth, deforestation, as well as flood- and drought related damages. To contour the endogeneity bias, we employ the three-stage least squares (3SLS) estimator with instrumental variables in our SEM as well as panel and mixed effect models as robustness checks.

Our results lend strong support to some interrelations of the supposed vicious cycle, while for others the evidence is more mixed and varies across world regions and development status. In particular, our findings suggest a strong link between urban expansion and tree cover loss at various spatial scales in all our specifications. This process is exacerbated by an increase in drought and flood damages which increase urban size in selected world regions, in particular Africa, Europe and North America. The impact of urban expansion on tree cover loss increases with the Human Development Index (HDI) in most world regions. Regarding the third link in the vicious cycle, we find that tree cover loss can either increase or attenuate flood and drought damages, depending on the context. It is therefore more pronounced in some regions than in others. Our evidence of the vicious cycle and its strength, dependent on the circumstances, holds insights for policymakers, which we discuss.

This study is organized as follows: In Section 2, we review some of the literature related to the urbanization, extreme events and deforestation nexus and derive hypotheses. This is followed by Section 3 describing the data sources, resolution as well as pre-processing and compilation, and Section 4, discussing the chosen model specification and estimation strategies. Section 5 comprises global average results as well as continent and HDI category specific results. The study concludes with a discussion and concluding remarks in Section 6.

# 2 Relation to the existing literature and hypotheses

There is a vast literature studying particular relations of interest in the extreme events - urbanization - tree cover loss nexus, often modeled in single equations. We build on many of these insights in the construction of our multi-equation estimation model.

## 2.1 Extreme weather events and urbanization

55% of the world population is now living in urban areas, with urbanization rates rising particularly fast in the developing world (United Nations, 2018). Among the pull-factors that drive migration from rural to urban areas, climate change patterns have in recent years been receiving particular attention. Moving is a key response to both slow-onset extreme events (such as droughts) and sudden-onset events (such as floods) (Kaczan and Orgill-Meyer, 2020). Examples of papers that show how climate events induce migration in individual countries include Gray and Mueller (2012) for Bangladesh, Joseph and Wodon (2013) for Yemen and Jessoe et al. (2018) for Mexico.

Barrios et al. (2006) and Marchiori et al. (2012) identify droughts as a key factor behind urbanization trends in Sub-Saharan Africa. Ober (2019) summarize the literature on the nexus between extreme events and migration in Asian countries. They also point out that the main movement is local, with most people migrating to nearby rather than faraway cities.

Castells-Quintana et al. (2021) work with global data to show that rainfall and temperature anomalies lead to an increase in urban rates across the whole hierarchy of cities and also change their internal structure. The effects are strongest in warmer and agriculture-based countries, in line with the mechanism outlined by Glaeser (2014) that urbanization increases with agricultural desperation.

While it is now a consensus in the literature that the effects of climatic change increase urbanization, Cattaneo and Peri (2016) find that the strength depends on the income level, because moving requires financial resources. The authors show that the effect is more pronounced in middle-income countries than in the poorest ones. This argument is corroborated by Peri and Sasahara (2019) with a global data set on population movements.

**Hypothesis 1**: Total economic damages from flood and drought events, are positively correlated with the rate of urbanization, particularly in agriculture-based and warmer countries, leading to an increase in urban size.

## 2.2 Urbanization and tree cover loss

The link between urbanization and tree cover loss has been an intensely debated topic. Cities often grow in area by expanding at the fringes. Natural habitats or agricultural land becomes urban space, leading to a loss in tree cover and biodiversity (van Vliet, 2019, Huang et al., 2018).

According to Behnisch et al. (2022), this process is driven by various factors, including institutional, economic, and demographic influences, and can persist even in regions with stagnant or declining populations. The authors find that globally, levels of urban expansion have rapidly increased between 1990 and 2014 and that urban expansion is positively associated with the Human Development Index.

On the other hand, Ecological Modernization Theory and the Environmental Kuznets Curve (EKC) suggest a nonlinear relation between urbanization - which goes in line with development - and tree cover loss, predicting that tree cover loss should decrease at higher stages of development.[1]

There have been various empirical studies confirming the existence of the EKC with peaks of deforestation at urbanization rates of 35% (Ehrhardt-Martinez et al., 2002) or 65% (Destiartono and Hartono, 2022), depending on the countries and time periods considered. Other studies fail to find such a connection (Koop and Tole, 1999). It is noteworthy that the EKC emphasizes the role of the rural population and its agricultural techniques for explaining deforestation, yet urban-based and global demands for agricultural products may be important drivers of deforestation as well (DeFries et al.,

[1]The EKC implies an inverted U-shaped relationship between urbanization as an indicator of the level of development and deforestation. It highlights the role of the rural population in deforestation: As described by Ehrhardt-Martinez et al. (2002), "slash- and burn agriculture" and high population growth during the early stages of economic development lead to deforestation. Later on, advanced farming techniques and reduced rural population pressure contribute to a slowdown in deforestation and, eventually, reforestation.

2010). According to the authors the notable trend of people migrating to tropical urban areas is likely to exert increased pressure on the clearance of tropical forests.

In summary, the impact of urbanization on tree cover is complex, as it is intertwined with the forces of economic development, resource extraction, and urban expansion. In contrast to the theoretical predictions of the EKC, empirical evidence suggests that urban growth, particularly when coupled with resource-intensive industries and expansive urban expansion, often leads to significant tree cover loss, with the extent and nature of this impact varying across different regions.[2] This leads to Hypothesis 2:

**Hypothesis 2**: Urban expansion significantly contributes to the loss of tree cover.

## 2.3 Tree cover loss and its impact on flood and drought damages

The third potential link to investigate goes from tree cover loss back to flood and drought damages to close the hypothetical vicious cycle.

It is widely acknowledged that forest ecosystems play a critical role in providing vital services such as carbon sequestration, biodiversity conservation, and climate regulation (MEA, 2005). The influence of forests on regulating extreme weather events, particularly floods and droughts, has received considerable attention in both scientific research and policy debates (van Dijk et al., 2009).

Mixed evidence exists regarding the adaptive capacity of forest cover in flood regulation. Several studies report that the loss of forest cover correlates with increased flood damages and a decline in flood mitigation capabilities (Bradshaw et al., 2007, Bhattacharjee and Behera, 2018, Tembata et al., 2020), and that changes in vegetation cover substantially modify the hydrological response in specific catchments (Costa et al., 2003). In contrast, other research suggests that tree cover loss does not significantly impact flood occurrence (Bowling et al., 2000, van Dijk et al., 2009) or alter the hydrological response and discharge in certain catchments (Beier et al., 2015, Kong et al., 2022).

Interestingly, van Dijk et al. (2009) challenge some of these findings by arguing that it is population density, rather than the clearance of forests, that predominantly influences flood damages following significant rainfall events. The authors emphasize the challenge of attributing flooding directly to tree cover loss without considering subsequent land use and its effect on soil infiltration capacity. This highlights the necessity of incorporating the subsequent land-use into our analysis when examining the impacts of forest cover loss. [3]

[2]Note that this is not necessarily a contradiction of the EKC for countries that are still on the upward-sloping part of the curve.

[3]A further important point to consider is potential heterogeneity in effects due to forest type, since

Regarding drought mitigation, the evidence in the literature is also mixed. Findings by Beier et al. (2015) indicate that loss of plant cover, when not followed by soil sealing, can be associated with enhanced drought mitigation.[4]

In contrast to that, long-term studies show that the forested Amazon basin, significantly influences regional rainfall patterns. The reduction in rain due to deforestation and consequent depletion of water vapor is linked to increasing drought events in Brazil (Nazareno and Laurance, 2015). In line with these findings, Smith et al. (2023) show that tree cover loss considerably reduced precipitation in various regions, impacting agriculture and hydropower generation and thereby intensifying drought damages.

Frenne et al. (2021) summarized findings indicating that tropical forests generate at least twice as much rain as areas with little or no vegetation. However, tree cover loss has to exceed a 30%-50% threshold to significantly reduce regional tropical rainfall. Lastly, Haile et al. (2019) point out that in East Africa, the aggravation of drought effects results from a combination of deforestation, land degradation, increasing water demand, and climate shifts.

Considering the breadth of evidence, it appears that while the relationship between tree cover loss and flood and drought regulation services is complex and influenced by various factors such as forest type and subsequent land use, there is a prevailing trend that suggests a reduction in tree cover tends to undermine an ecosystem's ability to regulate water, thereby potentially amplifying the impacts and damages of these extreme weather events. We thus hypothesize the following:

**Hypothesis 3**: Loss of tree cover is associated with increased damages from both floods and droughts due to the diminished capacity of affected ecosystems and related regulating services to regulate the damages from these extreme weather events.

If none of the hypotheses is rejected, this would mean that there exists a self reinforcing feed-back loop of extreme events, urbanization and tree cover loss.

Tembata et al. (2020) show that only broad leafed and mixed forest mitigated floods in China, while coniferous forests did not. Their results are also in line with Kong et al. (2022) who found only a low increase in catchment discharge after large-scale deforestation of German coniferous forest.

[4]In this particular case study and catchment in North America, de-vegetation lead to an increase in drought mitigation services that outweighed the loss of flood regulation services. When vegetation was removed, there was less water being absorbed by plants and less water lost to the atmosphere through the process of evapotranspiration. This means that more water remained in the soil or flowed into streams and rivers, thereby enhancing the availability of water during dry periods.

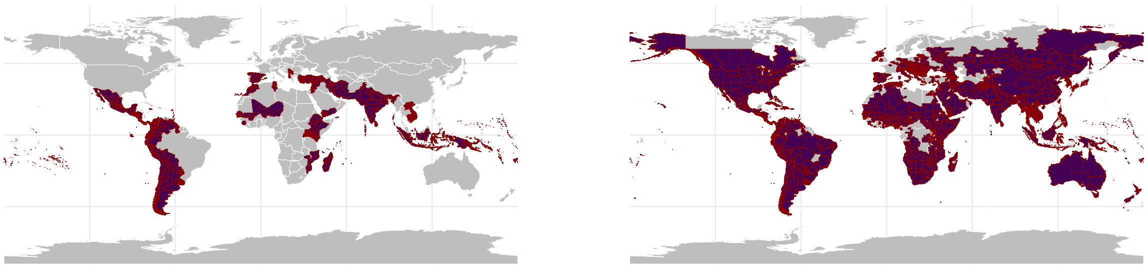

**(a)** Provinces DesInventar (2001-2013) **(b)** Provinces EM-DAT (2001-2018)

**Figure 1** – Included NUTS-1 regions with at least one flood or drought event in the respective time period in purple.

# 3 Data

For the estimation of our model, we meticulously compiled data from a variety of sources on an annual basis, aligning with NUTS-1 regional divisions. In our setting, NUTS-1 regions (corresponding to e.g. federal states in Brazil) are the most appropriate unit of observation. They strike the balance between availability of the different variables, ensuring a large number of observations, while at the same time having regions that are large enough to capture the effects of interest (e.g. urban expansion as a result of disaster-induced migration from the same region). The resulting spatial coverage of provinces is depicted in Figure 1.

Our units of observation are those NUTS 1 regions that experienced at least one flood or drought during the study period 2001-2018. We obtain this information, respectively, from the disaster data bases DesInventar (UNISDR, nd) and EM-DAT data (Guha-Sapir et al., 2009). Leveraging the administrative boundaries of these regions, we then calculated various variables using geo-spatial data. This process included aggregating information on the number of flood and drought events, associated fatalities, and total economic damages[5], as derived from the disaster data sets to an annual temporal resolution. We use two different datasets as our basis for the disaster data. The DesInventar dataset provides consolidated records of compiled information on disaster damages up until 2015 only for a selected number of countries - primarily from the developing world. We therefore expand our analysis using the EM-DAT database, which offers a more extensive temporal and spatial coverage, see Figure 1.

To account for differences in rural and urban contexts, we used the urban land cover class provided by ESA Land Cover CCI project team: Defourny (2019). Based on this class, we generated control variables such as population counts and nighttime lights both

[5]The EM-DAT's damage estimates include damages to infrastructure, crops, and housing.

for urban and rural areas in the identified provinces. We follow the literature in using nighttime lights as proxy for local economic activity and income (da Mata et al., 2012, Donaldson and Storeygard, 2016). We also include the number of victims of violent conflicts derived from Sundberg and Melander (2013), Davies et al. (2023) as a control variable.

Subsequently, we aggregated satellite land cover data to create variables indicative of land cover changes, as well as state variables such as the area of standing tree cover and bare ground. Our focus was particularly on tree cover loss stemming from all causes, but we only considered scenarios where there was no subsequent regrowth, resulting in bare or sealed surfaces. This approach allowed us to factor in the impacts of different land uses post tree cover loss. For an in-depth understanding of the data aggregation methods employed in our study, kindly refer to Table B-1, which outlines the aggregation framework. A comprehensive account of the variable generation process is provided in Appendix B.

The final data contains data on 1128 regions in 75 countries based on the DesInventar data and 2079 regions in 163 countries based on EM-DAT.

**Table 1** – Data Sources

| Data | Source |
|---|---|
| Disaster Loss Data | UNISDR (nd)<br>Guha-Sapir et al. (2009) |
| Land Cover | ESA Land Cover CCI project team: Defourny (2019) |
| Income Proxy | Li et al. (2020) |
| Population count | Global High Resolution Population Denominators Project (2018) |
| Conflict data | Sundberg and Melander (2013), Davies et al. (2023) |
| Administrative boundaries | FAO (2015) |
| Instrumental variables | ESA Land Cover CCI project team: Defourny (2019), Li and Xiao (2019), Liebmann and Smith (1996), Morice et al. (2021), Brakenridge (2016) |

Table 1 summarizes variable sources; Table A-1 in the Appendix provides an overview of all individual variables included.

# 4 Methods

## 4.1 Model specification

We specify a baseline model with four equations, based on the theoretical considerations, empirical findings and hypotheses derived from the literature described in Sections 2.1 to 2.3.

For the ease of exposition, we will here present the equations and the variables involved in a concise way. An overview over the variables, their hypothesized impact in each equation and the underlying literature can be found in Tables C-1 to C-2.

The first equation models the change in **city area** or size ($\Delta C$) as a function of various push and pull factors.

$$\begin{aligned}\Delta C = \alpha_1 + \beta_{11} LD_t + \beta_{12} LF_t \\ + \beta_{13} NTL_{U,t} + \beta_{14} P_{U,t} + \\ + \beta_{15} P_{nU,t} + + \beta_{16} NTL_{nU,t} + \\ \beta_{17} Ft_{C,t} + \beta_{18} TSB_t + u_1\end{aligned} \tag{1}$$

Push factors which potentially make people want to leave rural areas, include economic **losses from floods** ($LF_t$), **droughts** ($LD_t$), **fatalities** from violent **conflicts** ($Ft_{C,t}$), as well as **tree cover loss** with subsequent surface **sealing or bare** area ($TSB_t$)[6]. Pull factors are represented by mean **nighttime lights** in **urban** areas ($NTL_{U,t}$) as a proxy for income and economic activity in urban areas, compared to mean **nighttime lights** in **non-urban** areas ($NTL_{nU,t}$) representing economic incentives for rural-urban migration. Further control variables are **population counts** in **urban** ($P_{U,t}$) and **non-urban** areas ($P_{nU,t}$). The parameters $\alpha_1$ to $\beta_{18}$ represent the model coefficients, and $u_1$ the error term. Based on Hypothesis 1, we expect $\beta_{11}$ and $\beta_{12}$ to be positive. This would indicate that the economic losses experienced from flood and drought events act as a driver of urbanization.

The second equation relates to potential drivers and attenuation of **tree cover loss** with subsequent **surface sealing or bare area** ($TSB_t$).

$$\begin{aligned}TSB_t = \alpha_2 + \beta_{21} \Delta C + \beta_{22} T_t + \beta_{23} P_{nU,t} + \beta_{24} NTL_{nU,t} + \beta_{25} Cr_t \\ \beta_{26} S_t + \beta_{27} V_t + \beta_{28} B_t + \beta_{29} sealed \\ + \beta_{210} P_{U,t} + \beta_{211} NTL_{U,t} + \beta_{212} Ft_{C,t} + u_2\end{aligned} \tag{2}$$

This is modeled as a function of the change in **city area** ($\Delta C$), currently remaining **tree cover** ($T_t$), **other vegetation cover** ($V_t$), **shurb cover** ($S_t$), **bare surfaces** ($B_t$) and **sealed surfaces** ($sealed$).[7] The **population** count in **non-urban** areas ($P_{nU,t}$) is included with reference to the literature discussed in section 2.2, indicating that the

[6]Please refer to Appendix B for detailed information about the tree loss variable.

[7]Controlling for the variability of current land cover improves the accuracy and reliability of the model's estimates. It helps to reduce omitted variable bias, ensuring that the estimated coefficients for other variables are not confounded by the effects of land cover.

non-urban population can be a driver of tree cover loss due to activities like agriculture, logging, or other land uses that might impact tree cover. Mean **nighttime lights** in **non-urban** ($NTL_{nU,t}$) and **urban** areas ($NTL_{U,t}$) are included to proxy the level of economic development. Further included control variables comprise **crop cover** ($Cr_t$) to proxy agricultural practices and expansion, **urban population** count ($P_{U,t}$), and **fatalities** from violent **conflicts** ($Ft_{C,t}$).

Based on Hypothesis 2, we expect the model coefficient $\beta_{21}$ to be positive. In Equation (2) we test Hypothesis 2, suggesting that the net effect of urban expansion on tree cover loss is positive.

Equations (3) and (4) test the effect of tree loss with no subsequent vegetation regrowth on drought (Equation (3)) and flood damages (Equation (4)).

$$\begin{aligned} LD_t = \alpha_3 + \beta_{31}TSB_t + \beta_{32}Cr_t + \beta_{33}S_t + \beta_{34}T_t + \beta_{35}V_t + \\ + \beta_{36}D_t + \beta_{37}NTL_{nU,t} + \beta_{38}P_{nU,t} + \beta_{39}NTL_{U,t} + \beta_{310}P_{U,t} + u_3 \end{aligned} \tag{3}$$

$$\begin{aligned} LF_t = \alpha_4 + \beta_{41}TSB_t + \beta_{42}Cr_t + \beta_{43}S_t + \beta_{44}T_t + \beta_{45}V_t + \\ + \beta_{46}F_t + \beta_{47}NTL_{nU,t} + \beta_{48}P_{nU,t} + \beta_{49}NTL_{U,t} + \beta_{410}P_{U,t} + u_4 \end{aligned} \tag{4}$$

The third equation focuses on the economic losses from droughts ($LD_t$), while the fourth equation focuses on the economic losses from floods ($LF_t$). Both loss functions are modeled as a function of **tree cover loss** ($TSB_t$), as well as variables representing the non-sealed land cover such as **tree cover**($T_t$), **shrub cover** ($S_t$), other **vegetation** ($V_t$), **bare ground** ($B_t$) and **crop cover** ($Cr_t$). Furthermore, we use **population count** in **urban** and **non-urban** areas ($P_{U,t}, P_{nU,t}$), as well as the mean **nighttime light** in **urban** and **non-urban** areas ($NTL_{U,t}, NTL_{nU,t}$) to proxy exposure of assets, population, or systems that are at risk of being affected by floods or droughts. The number of **droughts** ($D_t$) in case of Equation (3) and the number of **floods** ($F_t$) in case of Equation (4) are included as a direct measure of the frequency of flood and drought events. The parameters $\alpha_3$, $\alpha_4$,$\beta_{31}$ to $\beta_{310}$ as well as $\beta_{41}$ to $\beta_{410}$ represent the two specifications' coefficients, $u_3$ and $u_4$ the error terms.

Based on Hypothesis 3, we expect $\beta_{31}$ and $\beta_{41}$ to be positive, indicating an increase in flood and drought related damages through the loss of tree cover and the related regulating potential.

## 4.2 Estimation strategy

In order to estimate our system of equations, we employ Simultaneous equation modeling (SEM). SEM is a robust statistical approach that is crucial for analyzing the interdependencies and potential feedback loops within the given context. It is widely employed to model relations between variables, for example in labor economics (Cai, 2010), development economics (Darda and Bhuiyan, 2022), politics (Evans and Pickup, 2010), and ecology (Fan et al., 2016), but we are unaware of SEM applications to study the extreme events - urbanization - deforestation nexus.

We use the *systemfit* R package (Henningsen and Hamann, 2007) to estimate our model's equations via the three-stage least square (3SLS) estimator, to address simultaneity bias. This bias arises when variables are used as both predictors and outcomes within the system. All our variables of interest are endogenous by definition of the SEM, since they enter the model both as dependent and explanatory variables. For example, the change in **city area** ($\Delta C$) is an outcome of equation (1) and a predictor of equation (2). The 3SLS method uses an instrumental variable approach to effectively correct the simultaneity bias. It also improves efficiency by accounting for the contemporaneous correlation among equation disturbances. Such a comprehensive approach ensures that the parameter estimates are both consistent and efficient, through the additional adjustment for bias due to omitted variables and measurement error by the use of instrumental variables (IVs) (Schmidt, 1990, Henningsen and Hamann, 2007). Identifying suitable IVs is critical in the following 3SLS modeling, as these must satisfy both exogeneity, i.e. being uncorrelated with the error terms[8] and relevance, i.e. having a strong correlation with the endogenous predictors (Wooldridge, 2012).

In the first stage IV Regression, the endogenous variables are predicted using the specified IVs (please refer to Table 2) and covariates for each equation:

$$LD_t = \delta_1 IV_{LD} + \beta_1 X_3 + v_1 \tag{5}$$

$$LF_t = \theta_1 IV_{LF} + \beta_2 X_4 + v_2 \tag{6}$$

$$TSB_{t,1} = \gamma_1 IV_{TSB1} + \beta_3 X_4 + v_3 \tag{7}$$

$$\Delta C = \pi_1 IV_{\Delta C} + \beta_4 X_1 + v_4 \tag{8}$$

$$TSB_{t,3} = \gamma_2 IV_{TSB3} + \beta_5 X_4 + v_5 \tag{9}$$

$$TSB_{t,4} = \gamma_3 IV_{TSB4} + \beta_6 X_4 + v_6 \tag{10}$$

where $IV$ represents the instrumental variable for the endogenous variable of the

[8] An IV is not correlated with the error term when it influences the dependent variable only through its direct effect on the explanatory variables that are endogenous.

respective equation and $X_i$ captures the vector of exogenous variables in equation $i$ in Section 4.1.

In the second stage, we substitute the predicted values of the endogenous variables back into their respective equations:

$$\Delta C = \alpha_1 + \beta_{11} L\hat{F}_t + \beta_{12} L\hat{D}_t + \beta_{13} Ft_{C,t} + \beta_{14} TS\hat{B}_{t,1} + \ldots + u_1 \tag{11}$$

$$TSB_t = \alpha_2 + \beta_{21} \Delta\hat{C} + \ldots + u_2 \tag{12}$$

$$LD_t = \alpha_3 + \beta_{31} TS\hat{B}_{t,3} + \ldots + u_3 \tag{13}$$

$$LF_t = \alpha_4 + \beta_{41} TS\hat{B}_{t,4} + \ldots + u_4 \tag{14}$$

Lastly, we estimate all equations simultaneously, accounting for the correlations among the disturbances:

$$\text{Minimize: } (\mathbf{Y} - \mathbf{X}\boldsymbol{\beta})'\Sigma^{-1}(\mathbf{Y} - \mathbf{X}\boldsymbol{\beta}) \tag{15}$$

$$\text{where: } \mathbf{Y} = \begin{bmatrix} \Delta C \\ TSB_t \\ LD_t \\ LF_t \end{bmatrix}, \quad \mathbf{X} = \text{Matrix of all explanatory variables incl. IVs,}$$

$$\boldsymbol{\beta} = \text{Vector of all coefficients}, \quad \Sigma = \text{Covariance matrix of residuals}$$

Table 2 displays the instruments used in the various specifications in this study. Due to the complexity of our analysis, which includes global and continental, as well as cluster-grouped analyses by continent and Human Development Index categories, multiple IVs are necessary. This is because different instruments are effective in different contexts, such as varying world regions, making it essential to utilize a diverse set of IVs to ensure robustness in our results. We test the strength of the instruments with F-tests of each of the equations used for the global analyses as well as for each of the sub-group analyses in Section 5. Depending on the results, one or several of the candidate instruments are included in the estimation procedure. The test results for the global models are available in Appendix D, while the remaining test results are available on request.

For the effect of drought damages on changes in urban size, we seek instruments that are related to environmental conditions or indicate drought vulnerability of the region but are not impacted by annual changes in urban areas. Depending on the respective sub-analysis, we use the annual mean temperature with an 8-year lag (Morice et al., 2021), the area of mixed treecover with a 9-year lag, the frequency of droughts, and the interaction between the area of crops with a 9-year lag and the frequency of droughts. These variables are all related to the vulnerability of a region to suffer drought damages

**Table 2** – 3SLS SEM Instrumental Variable Selection

| Dependent variable | Endogenous variable | Candidate instruments |
|---|---|---|
| $\Delta C$ | $LD_t$ | Mean temperature t-8, area of mixed treecover t-9, frequency of droughts, area of crops t -9 multiplied with frequency of droughts |
| | $LF_t$ | Outgoing longwave radiation, frequency of floods, area of crops t -9 multiplied with frequency of floods, flood frequency t- 4 and t- 8 |
| | $TSB_t$ | Tree cover loss with subsequent crop, shrub or other vegetation land cover t -9 |
| $TSB_t$ | $\Delta C$ | Area of sealed crop or shrub cover t- 9 |
| $LD_t$ | $TSB_t$ | Needle leafed tree cover loss with subsequent bare or sealed land cover t-9, Loss of unspecified tree cover to sealed land cover t- 9 |
| | | Area of needle leaved tree cover or sealed surfaces t- 9, Tree cover loss with subsequent crop or other vegetation land cover t- 9 |
| $LF_t$ | $TSB_t$ | see $LD_t$ |

and are thus significantly correlated with drought damages in $t$. The temporal lag of 8 to 9 years ensures the exogeneity of these instruments to a change in urban size in the current period. These drought patterns are shaped by long-term climate cycles and land cover dynamics rather than the immediate, year-to-year alterations in city size (Cook et al., 2018).

The land cover change from crop or shrub cover (Table B-1) to sealed surfaces with a temporal lag of nine years serves as an instrumental variable for $\Delta C$ in equation two as it is closely linked with urban expansion, which is typically a result of planned urban development influenced by political, economic, and demographic factors. This variable is chosen for its strong correlation with the urbanization process, as sealing surfaces is a direct and measurable consequence of urban growth. Crucially, it is plausibly exogenous to the specific process of tree cover loss leading to sealed or bare surfaces, as it reflects broader urban planning decisions rather than responses to tree cover status or changes.

The reasoning for selecting instruments for flood damages is similar. Changes in city size are generally too small to alter broader hydrological conditions that lead to flood occurence. Outgoing longwave radiation (OLR)[9], which correlates negatively with cloud coverage (Wang et al., 2002), and the frequency of floods with varying temporal lags depending on the region are therefore suitable instruments as they are related to larger-scale environmental patterns, or in the case of the area of crops with a temporal lag of nine years, multiplied with the frequency of floods a region's vulnerability to flood

[9]We use data by Liebmann and Smith (1996) to calculate the mean annual OLR.

damages and not to the year-to-year variations in urban expansion.[10]

As an instrument for tree cover loss without subsequent regrowth in the third and fourth equations we use tree cover loss with subsequent crop, shrub or other vegetation land cover with a temporal lag of nine years. These instruments capture other pathways of tree cover loss beyond urban expansion, such as deforestation for agricultural land use (Ehrhardt-Martinez et al., 2002), timber harvesting as well as other causes, such as wild fires.

Since the variable measures tree cover change from nine years prior, it is plausible to assume that it does not impact flood or drought damages in the present period of analysis. Therefore, it fulfills the exogeneity assumption necessary for valid instruments.

Since the data initially has a panel data structure, we apply the SEM on the country fixed-effects transformed data (Wooldridge, 2012). To test the robustness of our results, we estimate two further models in addition to the SEM: We estimate each equation separately using (i) a country and time fixed effects panel model with heteroskedasticity robust standard errors clustered at the continent level as well as (ii) a mixed effects model as robustness checks. In contrast to the SEM, these models cannot capture the interrelation of the four equations as a system, but they have other virtues. The panel model accounts for unobservable characteristics that are constant over time within a country (country fixed effects) and common effects across countries in each time period (year fixed effects), while accounting for potential intra-group correlations within continents, which is important if observations on the same continent are spatially correlated. The mixed effects model on the other hand allows for more complex error structures in nested data and can model both fixed effects, here defined as region and country fixed effects as well as random effects and thus address heterogeneity in the data better than the linear panel model.

# 5 Results

## 5.1 Global average results

Tables 3 and 4 display the results of the estimation described in Section 4. The first two columns show the results generated using the DesInventar data set, while the models presented in columns 3 and 4 respectively rely on the more comprehensive EM-DAT data. The results in the first and third columns were estimated by a 3SLS simultaneous equation model (SEM), which was applied to the fixed effects transformed data, while columns 2 and 4 display the results estimated with a panel model with country and year fixed effects, heteroskedasticity robust standard errors and clustered standard errors at

[10]Flood frequencies before the year 2000 were extracted from Brakenridge (2016).

the continent level (PLM).

Starting with **Hypothesis 1**, we find rather strong support across the data sets and models for a positive impact of economic damages from drought events ($LD_t$) on the change in urban size $\Delta C$. Only in the PLM model with the smaller Desinventar data set (column 2), the effect is not statistically significant from zero. By contrast, the association between economic flood damages ($LF_t$) and changes in city size presents a more complex picture, with significantly positive (PLM, EM-DAT), significantly negative (SEM, Desinventar) or insignificant coefficient estimates. Different effects in different world regions might contribute to this variation, and deserve a closer look in the heterogeneity analysis. We also note that the control variables included in Eq. (1) have the expected signs, e.g. urban nighttime lights $NTL_{U,t}$ as a pull factor are significantly positive and the non-urban nighttime lights as a push factor $NTL_{nU,t}$ are significantly negative across all models and data sets.

Turning to **Hypothesis 2**, we find strong support for a positive impact of a change of the urban size $\Delta C$ on tree cover loss $TSB$. The coefficient estimates are positive and statistically significant from zero at the 99% confidence level for all models and data sets.

Out of the three links we empirically investigate, the results provide least support for **Hypothesis 3**, respectively for the effect of tree cover loss $TSB$ on the economic drought $LD$ and flood damages $LF$. In the $LD$ regression, the SEM model applied to the EM-DAT data (column 3) is the only specification to yield a statistically significant, positive coefficient. The results in the other columns are positive or negative, but statistically insignificant. This variation in outcomes can be seen as indication for different mechanisms at play across ecological environments and world regions, which might cancel each other out in the global average. For the $LF$ regression, the effects of $TSB$ provide a similarly heterogeneous picture as for the $LD$ regression. The coefficients have positive or negative signs in different specifications but are never statistically significant from zero. Such disparities suggest that average results might mask important regional or context-specific variations, pointing to the need for more localized analyses to fully understand the complex dynamics behind Hypothesis 3.

We summarize the global average results about the links in the purported vicious cycle in Figure 2. We conclude that the evidence is strongest for the link from a change in urban size to deforestation (Hypothesis 2), while the other links are more ambiguous in the global sample of regions likely due to the heterogeneity we are going to analyze next.

**Table 3** – Global average results for Equations (1) and (2)

| | SEM | PLMFE | SEM | PLMFE |
|---|---|---|---|---|
| *Hypothesis 1:* Dep. variable: Change in city size $\Delta C_t$ | | | | |
| $LD_t$ | 1.1e-05 *** | 1.8e-07 | 2.0e-05 * | 1.6e-05 *** |
| | (1.1e-06) | (1.4e-07) | (9.0e-06) | (2.5e-06) |
| $LF_t$ | -2.7e-06 *** | 2.1e-08 | 2.9e-05 | 3.8e-06 *** |
| | (5.3e-07) | (4.4e-08) | (2.1e-05) | (8.3e-07) |
| $NTL_{U,t}$ | 6.6e-02 *** | 5.8e-02 *** | 2.3e-02 . | 2.2e-02 . |
| | (6.0e-03) | (5.5e-03) | (1.3e-02) | (1.3e-02) |
| $P_{U,t}$ | 2.5e-06 *** | 2.6e-06 *** | 5.0e-06 *** | 5.1e-06 *** |
| | (6.0e-08) | (5.4e-08) | (7.8e-08) | (7.3e-08) |
| $P_{nU,t}$ | 5.4e-07 *** | 5.3e-07 *** | 6.7e-07 *** | 7.3e-07 *** |
| | (1.3e-08) | (1.1e-08) | (5.3e-08) | (2.6e-08) |
| $NTL_{nU,t}$ | -9.2e-02 *** | -9.5e-02 *** | -2.1e-01 *** | -1.7e-01 *** |
| | (1.1e-02) | (1.0e-02) | (2.2e-02) | (2.2e-02) |
| $Ft_{C,t}$ | 2.2e-04 | 7.3e-05 | 2.1e-04 | 3.2e-04 |
| | (1.9e-04) | (1.9e-04) | (4.6e-04) | (4.6e-04) |
| $TSB_t$ | 4.0e-01 *** | 1.8e-01 *** | 3.1e-02 *** | 3.8e-02 *** |
| | (4.6e-02) | (1.3e-02) | (9.3e-03) | (3.6e-03) |
| | SEM | PLMFE | SEM | PLMFE |
| *Hypothesis 2:* Dep.variable: Tree cover loss $TSB_t$ | | | | |
| $\Delta C$ | 4.3e-01 *** | 8.3e-02 *** | 6.1e-01 *** | 7.5e-02 *** |
| | (1.3e-01) | (5.6e-03) | (1.0e-01) | (6.5e-03) |
| $T_t$ | 5.5e-06 *** | 6.1e-06 *** | 1.0e-04 *** | 9.9e-05 *** |
| | (1.2e-06) | (1.2e-06 ) | (1.1e-06) | (9.1e-07) |
| $P_{nU,t}$ | -2.0e-07 *** | -3.8e-08 *** | -4.2e-07 *** | 7.2e-08 . |
| | (5.6e-08) | (9.3e-09) | (1.2e-07) | (3.7e-08) |
| $NTL_{nU,t}$ | 4.6e-02 *** | 1.6e-02 * | 2.0e-01 *** | 8.5e-02 *** |
| | (1.2e-02) | (6.6e-03) | (3.0e-02) | (2.6e-02) |
| $Cr_t$ | -5.5e-06 . | -1.1e-06 | -4.6e-05 *** | -7.1e-05 *** |
| | (3.3e-06) | (2.1e-06) | (1.2e-05) | (6.5e-06) |
| $S_t$ | -4.1e-07 | 5.4e-07 | 1.3e-05 . | 2.8e-05 *** |
| | (2.0e-06) | (1.9e-06) | (7.2e-06) | (4.2e-06) |
| $V_t$ | 1.9e-05 *** | 1.4e-05 *** | 2.3e-05 *** | 1.4e-05 *** |
| | (4.1e-06) | (1.5e-06) | (4.1e-06) | (2.4e-06) |
| $B_t$ | 2.9e-07 | 1.9e-07 | 9.1e-06 ** | 9.1e-06 ** |
| | (9.3e-07) | (9.3e-07) | (3.0e-06) | (3.0e-06) |
| sealed | -2.1e-03 * | -6.8e-04 *** | -1.8e-03 * | -4.7e-05 |
| | (1.1e-03) | (1.7e-04) | (7.5e-04) | (1.5e-04) |
| $P_{U,t}$ | -6.7e-07 *** | 4.2e-10 | -1.9e-06 *** | 1.8e-08 |
| | (1.6e-07) | (4.3e-08) | (2.3e-07) | (1.1e-07) |
| $NTL_{U,t}$ | -3.1e-02 *** | -9.7e-03 ** | -1.9e-03 | 1.7e-02 |
| | (8.3e-03) | (3.6e-03) | (1.6e-02) | (1.5e-02) |
| $Ft_{C,t}$ | -1.4e-04 | -7.1e-05 | -7.3e-06 | 3.9e-05 |
| | (1.3e-04) | (1.2e-04) | (5.5e-04) | (5.4e-04) |
| Data | Desinventar | | EM-DAT | |
| N | 15,451 | | 36,938 | |
| Years | 2001-2013 | | 2001-2018 | |

3SLS estimation of the simultaneous equation model with instrumental variables (SEM) on the demeaned transformed data compared to the results of panel model estimation with country and time fixed effects, heteroskedasticity robust standard errors and clustered standard errors at the continent level (PLMFE) across datasets. Coefficient estimates are presented with standard errors in parentheses. * $p < 0.05$, ** $p < 0.01$, *** $p < 0.001$.

**Table 4** – Global average results for Equations (3) and (4)

| | SEM | | PLMFE | | SEM | | PLMFE | |
|---|---|---|---|---|---|---|---|---|
| *Hypothesis 3:* Dep. variable: Economic Drought Damages $LD_t$ | | | | | | | | |
| $TSB_t$ | 1.5e+01 | | -2.7e+01 | | 1.4e+02 | *** | -1.7e+01 | |
| | (2.6e+03) | | (7.5e+02) | | (3.7e+01) | | (8.7e) | |
| $Cr_t$ | 8.7e-01 | *** | -1.3e-01 | | 1.7e-02 | | 6.6e-03 | |
| | (1.6e-01) | | (1.7e-01) | | (1.1e-02) | | (1.0e-02) | |
| $S_t$ | 2.1e | *** | 2.1e | *** | 5.9e-02 | *** | 6.3e-02 | *** |
| | (1.7e-01) | | (1.8e-01) | | (7.0e-03) | | (6.9e-03) | |
| $T_t$ | -6.4e-02 | | 5.5e-02 | | -1.9e-02 | *** | -4.1e-03 | * |
| | (1.0e-01) | | (1.1e-01) | | (3.9e-03) | | (1.8e-03) | |
| $V_t$ | -1.2e | *** | -1.1e | *** | -4.5e-03 | | -1.8e-03 | |
| | (1.3e-01) | | (1.3e-01) | | (3.5e-03) | | (3.4e-03) | |
| $D_t$ | 4.3e+03 | *** | 4.0e+03 | *** | 8.5e+04 | *** | 8.4e+04 | *** |
| | (4.7e+02) | | (5.0e+02) | | (1.2e+03) | | (1.2e+03) | |
| $NTL_{nU,t}$ | -1.8e+02 | | -5.6e+02 | | -1.8e+02 | *** | -1.8e+02 | *** |
| | (5.8e+02) | | (5.9e+02) | | (4.3e+01) | | (4.3e+01) | |
| $P_{nU,t}$ | -3.7e-03 | *** | -1.1e-03 | | 2.6e-05 | | 4.7e-05 | |
| | (7.8e-04) | | (8.0e-04) | | (6.0e-05) | | (6.0e-05) | |
| $NTL_{U,t}$ | -1.3e+01 | | 4.6e+01 | | 6.3e+01 | * | 5.2e+01 | * |
| | (3.2e+02) | | (3.2e+02) | | (2.5e+01) | | (2.5e+01) | |
| $P_{U,t}$ | 5.3e-03 | . | 7.2e-03 | * | 4.6e-04 | ** | 5.0e-04 | *** |
| | (3.1e-03) | | (3.1e-03) | | (1.5e-04) | | (1.5e-04) | |
| | SEM | | PLMFE | | SEM | | PLMFE | |
| *Hypothesis 3:* Dep. variable: Economic Flood Damages $LF_t$ | | | | | | | | |
| $TSB_t$ | 7.3e+03 | | -4.6e+02 | | 2.0e+02 | . | -1.5e+01 | |
| | (8.5e+03) | | (2.5e+03) | | (1.1e+02) | | (2.8e+01) | |
| $Cr_t$ | -2.5e | *** | -2.0e-01 | | 1.3e-01 | *** | 1.8e-01 | *** |
| | (5.5e-01) | | (5.7e-01) | | (3.3e-02) | | (3.3e-02) | |
| $S_t$ | -2.3e-01 | | -1.8e-01 | | 8.2e-02 | *** | 5.9e-02 | ** |
| | (5.6e-01) | | (5.8e-01) | | (2.1e-02) | | (2.2e-02) | |
| $T_t$ | -8.8e-02 | | -3.3e-01 | | -8.4e-03 | | 2.1e-02 | *** |
| | (3.5e-01) | | (3.6e-01) | | (1.2e-02) | | (5.6e-03) | |
| $V_t$ | 6.5e-01 | | 4.2e-01 | | -9.7e-02 | *** | -1.2e-01 | *** |
| | (4.2e-01) | | (4.3e-01) | | (1.1e-02) | | (1.1e-02) | |
| $F_t$ | 3.3e+03 | *** | -1.6e+01 | | 8.2e+04 | *** | -1.1e+04 | ** |
| | (1.0e+03) | | (1.6e+03) | | (1.7e+03) | | (3.9e+03) | |
| $NTL_{nU,t}$ | -1.9e+03 | | -1.0e+03 | | 2.5e+02 | . | 7.5e+01 | |
| | (1.9e+03) | | (1.9e+03) | | (1.3e+02) | | (1.4e+02) | |
| $P_{nU,t}$ | 9.8e-03 | *** | 3.9e-03 | | 1.2e-03 | *** | 1.6e-03 | *** |
| | (2.6e-03) | | (2.6e-03) | | (1.8e-04) | | (1.9e-04) | |
| $NTL_{U,t}$ | 5.0e+02 | | 4.1e+02 | | -1.1e+01 | | 2.3e+01 | |
| | (1.0e+03) | | (1.1e+03) | | (7.8e+01) | | (8.1e+01) | |
| $P_{U,t}$ | -1.4e-02 | | -1.5e-02 | | -3.7e-05 | | 5.9e-04 | |
| | (1.0e-02) | | (1.0e-02) | | (4.5e-04) | | (4.6e-04) | |
| Data | Desinventar | | | | EM-DAT | | | |
| N | 15,451 | | | | 36,938 | | | |
| Years | 2001-2013 | | | | 2001-2018 | | | |

3SLS estimation of the simultaneous equation model with instrumental variables (SEM) on the demeaned transformed data compared to the results of panel model estimation with country and time fixed effects, heteroskedasticity robust standard errors and clustered standard errors at the continent level (PLMFE) across datasets. Coefficient estimates are presented with standard errors in parentheses. * $p < 0.05$, ** $p < 0.01$, *** $p < 0.001$.

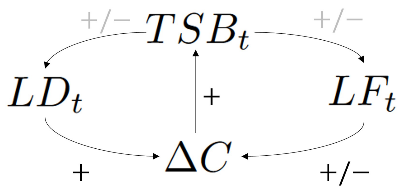


**Figure 2** – Synthesis of global average results.

## 5.2 Heterogeneous effects

How does the hypothetical vicious cycle - and the strength of its links - vary across world regions? Since intuition as well as the global average results point towards (spatial) heterogeneity in effects, we conducted the SEM analysis using EM-DAT for each continent.[11] As the urban expansion and EKC literature suggest results might vary dependent on the economic/human development (Ehrhardt-Martinez et al., 2002, Behnisch et al., 2022), Figure D-6 displays heterogeneity across Human Development categories. We categorize the regions in our data by Human Development Index (HDI) based on United Nations Development Programme (2024) and consolidate the high and very high HDI categories into a single category.[12] Please refer to Figures A-2 and A-3 for an overview of the HDI categories across regions at the start and at the end of the study period.

### 5.2.1 Analysis of heterogeneity in results across continents

In Figure 5.2.1, we show the spatial heterogeneity in results categorized by continent.[13]

**Hypothesis 1**, which had received rather strong support in the global average analysis, nevertheless comes with considerable spatial heterogeneity. The positive effect of drought damages on change in urban size (Figure 3a) seems to be most strongly driven by Africa and North America, while it is weakly negative in Europe. By contrast, we find a significantly positive link from economic flood damages on change in urban size (Figure 3b) on all continents except South America. Hence, on a continent-level the link from flood damages to urban expansion is stronger than the global average results suggest.

For **Hypothesis 2**, which was unambiguous in the global average results, we also find very strong support across regions (Figure 3c). The coefficients of the effect from urban expansion on tree cover loss are positive and highly statistically significant in every individual region. They are of highest magnitude in Europe, North America and Africa.

[11] Since the DesInventar data is more limited and has a clear focus on the Global South, we use the EM-DAT data for this analysis, as this data covers regions in more countries, including the Global North.

[12] The HDI categories are low (HDI $< 0.550$), medium ($0.550 \leq$ HDI $\leq 0.699$), high (HDI $\geq 0.700$), and very high (HDI $\geq 0.800$). Note that the categorization is by region; in particular middle-income countries may have some high and low HDI regions.

[13] These results based on SEM estimation are complemented by robustness checks for each continent and variable of interest using a two-way fixed effects estimator as well as a mixed effects models as robustness checks, shown in Figures D-1 to D-5.

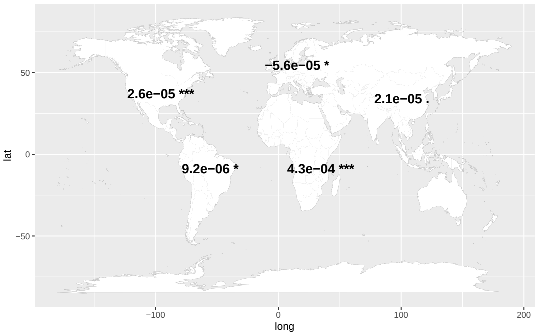


**(a)** $\Delta C \leftarrow LD_t$ (H1)

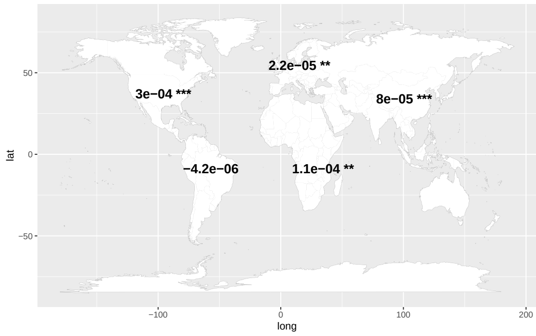


**(b)** $\Delta C \leftarrow LF_t$ (H1)

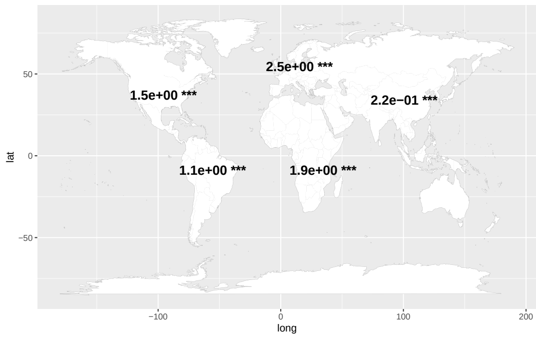


**(c)** $TSB_t \leftarrow \Delta C$ (H2)

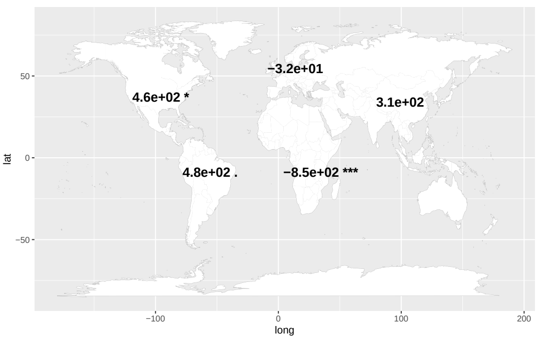


**(d)** $LD_t \leftarrow TSB_t$ (H3)

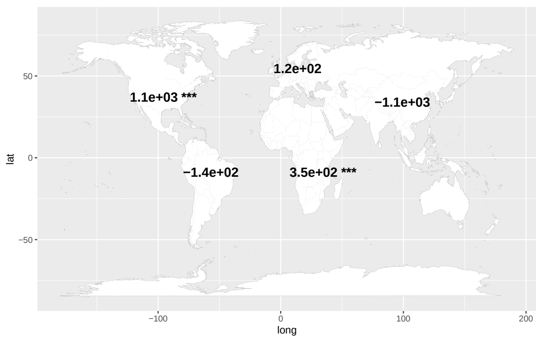


**(e)** $LF_t \leftarrow TSB_t$ (H3)

**Figure 3** – Continent level model effects based on the EM-DAT data set estimated with an 3-sls simultaneous equation model on the transformed data.Transformation: Fixed effects transformation to account for panel structure of the data (Wooldridge, 2012). . $p < 0.10$, * $p < 0.05$, ** $p < 0.01$, *** $p < 0.001$

Concerning **Hypothesis 3**, the insignificant global average results seem to be a composition effect of opposite results across continents. In North America, tree cover loss has a significantly positive effect on economic drought damages (Figure 3d), while the effect is negative in Africa. As we will discuss later, this heterogeneity in effects might go in line with the different ecological environments and varying types of trees. Similarly, the effect of tree cover loss on economic flood damages (Figure 3e) varies across continents. They are positive and significant in Africa and North America in the SEM specification[14], while the sign is negative in Asia (and statistically significant in most models, see Figure D-3).

In sum, the results indicate that the complete vicious cycle with regard to drought damages is most strongly discernible in North America and with regard to flood damages in Europe and Africa.

A heterogeneity analysis on continent level is, however, limited since it does not fully address heterogeneity with respect to human development as an important factor in collective and individual adaptation potential. Thus we proceed to Section 5.2.2.

### 5.2.2 Analysis of heterogeneity across Human Development categories

Besides the heterogeneity of results across continents, our findings also indicate that the Human Development Index is a key factor in explaining the variation in results. Based on the point estimates of the variables of interest across estimation strategies displayed on Figure D-6, we identified the following mechanisms for each HDI category as shown on Figure 4:

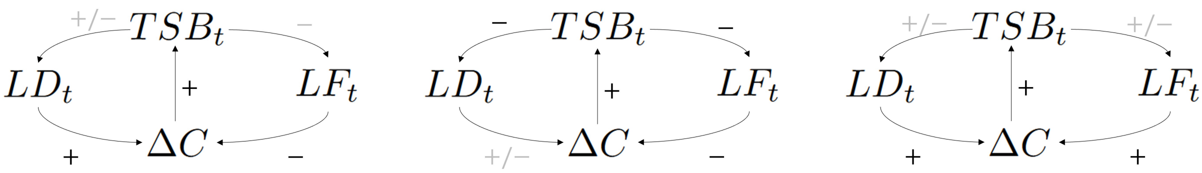


**(a)** Low HDI **(b)** Medium HDI **(c)** High and very High HDI

**Figure 4** – Results across Human Development Index (HDI). Conclusive coefficient estimates across estimation strategies with at least one strategy showing a statistically significant effect are displayed by a black sign, whereas the grey sign indicates exclusively insignificant coefficients.

Across all HDI categories, we find strong evidence of the link from urban expansion to tree cover loss (Hypothesis 2), confirming our insights from the global averages and continent-level analysis. The urban expansion process is reinforced by drought damages (Hypothesis 1) in the low and high and very high HDI categories, while the results are mixed in the medium HDI category. Flood damages, by contrast, have a positive effect

[14] The results for North America concerning the effect of tree cover loss on flood damages are however not robust across specifications.

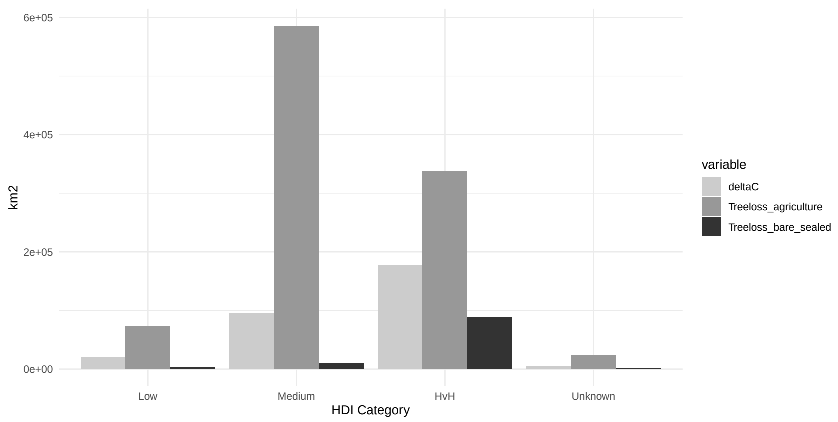


**Figure 5** – Observed conversion of tree cover to bare and sealed or agricultural surfaces and urban expansion categorized by Human Development Index between 2001-2018 based on ESA Land Cover CCI project team: Defourny (2019).

on urban expansion (Hypothesis 1) in regions with a high or very high HDI and decrease urban expansion in regions with a low to medium HDI. Again, the effect of tree cover loss without subsequent regrowth on damages (Hypothesis 3) contains most heterogeneity, also across HDI categories. This points towards context specific regulation capacity and ecosystem services driven by other factors than human development, as is also evident from the continent-level results in the previous sub-section.

We sub-categorize the data further by combining the human and environmental sources of heterogeneity, in particular HDI and the continent.[15]. Focusing on the hypothesis with the most ambiguous results (Hypothesis 3), we see a positive effect of tree cover loss on drought damages in low HDI African and high and very high HDI North American regions, however these results are statistically insignificant. For the impact of tree cover loss on flood damages, we find a positive coefficient in high and and very high HDI European, and African regions as well as in low and medium HDI North American regions, where only the results for Europe and Africa are statistically significant. The absolute effect of urban expansion on tree cover loss is increasing with HDI on all continents except South America (where the effect is highest in the medium HDI category), see D-7c. In Figure 5, we see that conversion of tree cover with subsequent agricultural use follows a kind of inverted U-shape depending on HDI category as one would expect based on the EKC literature. However, urban expansion and tree cover loss with subsequent bare or sealed land cover increase with human development.

Concluding our heterogeneity analysis, we look for those combinations of continent and HDI where we find the most pronounced vicious cycles. Figure 6 displays the vicious cycles with the strongest effects and where we cannot reject the three hypotheses for either drought or flood events. Regions with such a pronounced vicious cycle can be

[15]Please refer to Appendix Figure D-7 for the point estimates of all variables of interest clustered by continent and HDI

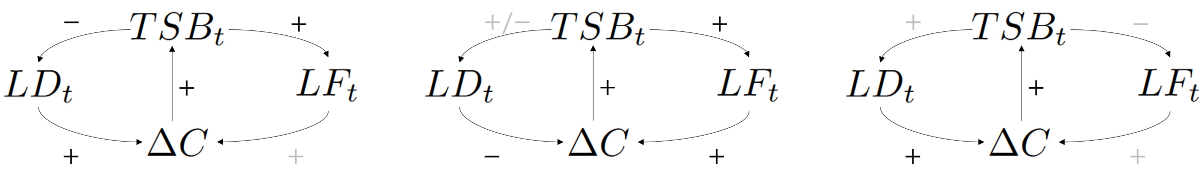


**(a)** High HDI African regions **(b)** High HDI Europe **(c)** High HDI North America

**Figure 6** – Selected results across Human Development Index (HDI) and Continents. Note: The high HDI category in this study subsumes the high and very high HDI categories defined by the UNDP. Significant effects are displayed by a black sign, whereas the grey sign indicates insignificant coefficients.

found on various continents (Africa, Europe, North America), but it is conspicuous that the regions involved have a high HDI.

# 6 Discussion and Conclusions

In this study, we investigated the complex interplay between flood and drought damages, their impact on urban growth, the influence of urban expansion on tree cover loss, and how this, in turn, affects the severity of flood and drought damages. To investigate the presence of this vicious cycle, we employed econometric methods on two compiled data sets with varying spatial and temporal coverage. As the first study investigating this interrelation by estimating a system of four equations, we explicitly modeled the impact of human behavior in the form of land-use changes due to urban expansion, along with the ensuing environmental consequences related to the climate regulation services provided by tree-based ecosystems, and resulting costs for society in the form of economic damages of extreme weather events. We have found evidence of the existence of the vicious cycle at the global scale, yet some links are stronger than others. Our results most strongly support the link from urban expansion to tree cover loss, and from drought damages to urban expansion. There is more spatial heterogeneity for the role of tree cover loss in attenuating or amplifying drought damages. Our sub-analyses show that this vicious cycle with respect to drought damages is particularly pronounced in North American regions with a high HDI. With respect to flood damages, the vicious cycle is most evident in European regions with high HDI, as well as in African regions with high HDI.

This leads to the question of the underlying mechanisms, in particular the role of economic development. Previous studies focusing on droughts and floods as the drivers of urbanization (Hypothesis 1) have highlighted the role of rural to urban migration (Cattaneo and Peri, 2016, Ober, 2019, Peri and Sasahara, 2019). This migration channel typically applies for poor and middle-income countries and can be thought to contribute to our strong results on the link from drought to urban expansion in Africa, including high HDI African regions.[16] It should be noted, however, that population growth in cities also leads to a densification, particularly in low-income countries (Castells-Quintana et al., 2021). Here we measure the increase in the urban extent because it matters for the land use tradeoff and resulting deforestation. If the additional population from rural to urban migration is primarily absorbed by densifying existing urban areas (e.g. with informal settlements), it will not expand the urban area. This might explain why we find stronger support for the urban expansion link in high HDI rather than low HDI African regions. At the same time, rural to urban migration is unlikely to be the driving force behind the corresponding results for Europe and North America. Different urban planning policies and suburbanization might play a role; in fact, Behnisch et al. (2022) observe urban expansion even in high-HDI areas without population growth, sometimes even where population declines. Demand for housing and commercial space is driven towards the urban outskirts, facilitated by zoning regulations that favor urban expansion over densification in high-HDI countries (Behnisch et al., 2022). According to Ehrlich et al. (2018), institutional fragmentation might be another factor facilitating urban expansion and concurrent surface sealing in selected high-HDI regions. These tendencies can be intensified by severe floods and droughts as we measure them. In high HDI regions the comparatively higher insurance coverage and resulting insurance claims, particularly in Europe and the USA (Allianz Global Corporate & Specialty, 2017) might lead to rebuilding efforts that do not only restore but expand pre-disaster infrastructure and housing also in the urban fringe. This link might be weaker in low and medium HDI areas with less insurance cover. In fact, there might even be statistical undercounting of economic damages of extreme events for this reason, which might contribute to the weaker evidence of the link from economic damages of floods and droughts to urban expansion in low HDI regions.

Our unambiguous findings of urban expansion increasing tree cover loss (Hypothesis 2) also warrant some discussion. This relationship intensifies with an increase in the HDI (except in South America). This suggests a more intricate relationship than the Environmental Kuznets Curve theory proposes, where deforestation is expected to decline at higher levels of development (Ehrhardt-Martinez et al., 2002). As we have shown, in our data the conversion from tree-based systems to agricultural areas exceeded the conversion to bare and sealed surfaces between 2001 and 2018, indicating that tree cover loss with no regrowth is still lower in absolute terms in the high and very high HDI categories compared to the medium HDI category. Urban expansion, however, might

[16] African regions with a high HDI include metropolitan regions in Maghreb countries (Tunis in Tunisia, Grand Casablanca in Morocco), tourism-based regions (Port Louis on Mauritius) and export-oriented regions (Western Cape in South Africa, various gas-exporting Algerian regions).

be a stronger driver of the conversion to sealed area, and it is more important in high HDI regions than in the other HDI categories. Moreover, increasing population pressure and increasing human development across the globe can be thought to impact this relationship in the long run. DeFries et al. (2010) argues that urban demands also across borders and continents drive conversion of tree cover to agricultural areas especially in the Global South. This stresses that the EKC is a correlational construct and does not justify the assumption that increasing human development solves the problem of tree cover loss.

It is line with the literature that our findings on the link from tree cover loss to economic damages of floods and droughts (Hypothesis 3) vary less systematically with HDI but more with the continent and the dominating ecological environment (Beier et al., 2015, van Dijk et al., 2009, Bradshaw et al., 2007). Since we specifically focus on tree loss with subsequent surface sealing or bare land cover we capture processes that are detrimental to the existing ecological functions of the respective parcel of land that is cleared and sealed; a process difficult to reverse (Scalenghe and Marsan, 2009, Tobias et al., 2018). Such sealing, as highlighted in our study, can create a scenario where the ecological balance is not just temporarily disturbed but fundamentally reshaped, often with long-term negative impacts on biodiversity and ecosystem services. In line with van Dijk et al. (2009), our study design and resulting nuanced findings clearly emphasize the importance of delineating the specific forms of tree cover loss being examined and consider land cover post tree cover loss.

Our study has some limitations that are worth discussing. Working with worldwide regional data, sets the focus on breadth which necessarily comes at the expense of depth. In particular, investigating the loss of tree cover due to urban expansion and the associated regulating services at the aggregated province (NUTS 1) level poses several challenges. Firstly, at this scale, there is a risk of oversimplifying complex environmental dynamics, as the heterogeneity in drivers and ecosystem functions within regions may be masked. Secondly, the aggregation process can lead to a loss of fine-grained, local information about land cover distribution, which may be crucial for understanding how specific ecosystems interact with and provide regulating services to their immediate surroundings. This aggregated approach may miss subtle but significant variations in land-use patterns and their impacts on regulating services, potentially overlooking critical nuances in ecosystem functioning. Regional studies focusing on specific areas in detail can obviously take these particularities better into account and offer insights that are more pertinent to individual regions. However, analyzing the nexus between extreme weather events, urban expansion, and tree cover loss on a global scale with continent- and HDI-specific sub-analyses, as we did in this study, offers the advantage of providing a comprehensive, policy-relevant understanding of these complex interactions, while also enabling the identification of global hotspots. Furthermore, the literature discussed in section 2.3, finds that tree cover loss has a spatial lag when affecting drought damages. According to Smith et al. (2023), the effects of tree cover loss might manifest themselves in distances of up to hundreds or thousand kilometers away from the original place of deforestation. Thus, we consider aggregating the available data at the NUTS 1 level and combining this with a multi-level analysis as a sensible approach in this context. Yet, it should be noted that spatial spillovers to other regions are not specifically considered in our approach (beyond controlling for their impact on spatial error correlation). A more nuanced analysis of spillovers between regions would be an interesting avenue for future research.

A further caveat relates to the data quality. The heterogeneity in our results, could be partly attributed to the limitations in the disaster data used, specifically the damage estimates which are not consequently reported for all drought and flood events and might also vary in the degree to which they are consistently documented in regions across HDI categories[17] By working with two different data sets, we try to minimize this drawback. At the same time, data quality is always an issue in global studies of this scope. For instance, the definition of urban or sealed land cover in this study relies both on the definition of urban areas in Commission et al. (2016) and on DLR (2016) and the results of this study should be interpreted in this context, exclusively.

Despite these caveats, our results on the vicious cycle and its strength across continents and income levels provides valuable results for policymakers. Even though some national and supranational governments acknowledge the sustainability challenges of urban expansion (European Environment Agency, 2016) and have set in place containment policies - some European countries, have for instance set a targets for limiting land consumption for residential purposes and infrastructure development- there are rarely mechanisms in place to ensure that the targets are met (Bovet et al., 2018). In the face of urban expansion, setting realistic containment targets and establishing effective incentives is crucial for policymakers to balance land preservation with development needs. Beyond just the regulation of land use, a holistic approach is necessary to address the broader spectrum of sustainability objectives, since limiting urban sprawl may incur trade-offs with housing affordability (Bovet et al., 2018). In conclusion, our study underscores the intricate relationship between urban expansion, tree cover loss, and their impacts on flood and drought damages on the global average and its regional particularities. Our findings highlight the critical need for nuanced, region-specific policies which acknowledge the

[17] Panwar and Sen (2020), highlight that the two disaster datasets we used in this study, which vary extensively in spatial and temporal coverage, often present considerable discrepancies in reported damage estimates. This variability underscores the challenges in obtaining consistent and reliable disaster data.

complex dynamics of urban expansion, tree cover loss, and their interplay with natural disasters. As urbanization continues to accelerate globally, understanding and addressing these feedbacks is crucial to mitigate the negative effects on ecosystems and human society.

# References


Adams, H. and W. N. Adger (2013, 3). The contribution of ecosystem services to place utility as a determinant of migration decision-making. *Environmental Research Letters 8*, 015006.

Allianz Global Corporate & Specialty (2017). Global claims review: Liability in focus - loss trends and emerging risks for businesses. https://commercial.allianz.com/content/dam/onemarketing/commercial/commercial/reports/AGCS-Global-Claims-Review-2017.pdf. Accessed: [13.03.2024].

Barrios, S., L. Bertinelli, and E. Strobl (2006). Climate Change and Rural-Urban Migration: the Case of Sub-Saharan Africa. *Journal of Urban Economics 26*, 656–673.

Baum-Snow, N. and R. Pavan (2011, 08). Understanding the City Size Wage Gap. *The Review of Economic Studies 79*(1), 88–127.

Behnisch, M., T. Krüger, and J. A. G. Jaeger (2022, 11). Rapid rise in urban sprawl: Global hotspots and trends since 1990. *PLOS Sustainability and Transformation 1*, e0000034.

Beier, C. M., J. Caputo, and P. M. Groffman (2015, 10). Measuring ecosystem capacity to provide regulating services: Forest removal and recovery at hubbard brook (usa). *Ecological Applications 25*, 2011–2021.

Bhattacharjee, K. and B. Behera (2018, 11). Does forest cover help prevent flood damage? empirical evidence from india. *Global Environmental Change 53*, 78–89.

Bluhm, R. and M. Krause (2022). Top lights: Bright cities and their contribution to economic development. *Journal of Development Economics 157*, 150.

Bovet, J., M. Reese, and W. Köck (2018). Taming expansive land use dynamics – sustainable land use regulation and urban sprawl in a comparative perspective. *Land Use Policy 77*, 837–845.

Bowling, L. C., P. Storck, and D. P. Lettenmaier (2000). Hydrologic effects of logging in western washington, united states. *Water Resources Research 36*, 3223–3240.

Bradshaw, C. J., N. S. Sodhi, K. S. Peh, and B. W. Brook (2007, 11). Global evidence that deforestation amplifies flood risk and severity in the developing world. *Global Change Biology 13*, 2379–2395.

Brakenridge, G. (2016). Global active archive of large flood events. http://floodobservatory.colorado.edu/Archives/. Accessed 29 February 2024.

Cai, L. (2010). The Relationship Between Health and Labor Force Participation: Evidence from a Panel Data Simultaneous Equation Model. *Labour Economics 17*(1), 77–90.

Camargo, G., A. M. Sampayo, A. P. Galindo, F. J. Escobedo, F. Carriazo, and A. Feged-Rivadeneira (2020, 11). Exploring the dynamics of migration, armed conflict, urbanization, and anthropogenic change in colombia. *PLOS ONE 15*, e0242266.

Castells-Quintana, D., T. McDermott, and M. Krause (2021). The Urbanising Force of Global Warming: The Role of Climate Change in the Spatial Distribution of Population. *Journal of Economic Geography 21*(4), 531–556.

Cattaneo, C. and G. Peri (2016). The Migration Response to Increasing Temperatures. *Journal of Development Economics 122*, 127–146.

Christiansen, R., M. Baumann, T. Kuemmerle, M. D. Mahecha, and J. Peters (2022, 4). Toward causal inference for spatio-temporal data: Conflict and forest loss in colombia. *Journal of the American Statistical Association 117*, 591–601.

Commission, E., J. R. Centre, P. Soille, M. Halkia, S. Freire, S. Ferri, A. Julea, M. Pesaresi, T. Kemper, D. Ehrlich, V. Syrris, and A. Florczyk (2016). *Operating procedure for the production of the global human settlement layer from Landsat data of the epochs 1975, 1990, 2000, and 2014*. Publications Office.

Cook, B., J. Mankin, and K. Anchukaitis (2018). Climate Change and Drought: From Past to Future. *Current Climate Change Reports 4*, 164–179.

Costa, M. H., A. Botta, and J. A. Cardille (2003, 12). Effects of large-scale changes in land cover on the discharge of the tocantins river, southeastern amazonia. *Journal of Hydrology 283*, 206–217.

D. da Mata, U. Deichmann, J.V. Henderson, S.V. Lall, and H.G. Wang (2007). Determinants of city growth in brazil. *Journal of Urban Economics 62*(2), 252–272.

da Mata, D., U. Deichmann, J. Henderson, S. Lall, and H. Wang (2012). Measuring Economic Growth from Outer Space. *American Economic Review 102*(2), 994–1028.

Darda, M. A. and M. A. H. Bhuiyan (2022). A Structural Equation Model (SEM) for the Socio-Economic Impacts of Ecotourism Development in Malaysia. *PlosOne*, 0273294.

Davies, S., T. Pettersson, and M. Öberg (2023). Organized violence 1989-2022 and the return of conflicts between states? *Journal of Peace Research 60*(4).

DeFries, R. S., T. Rudel, M. Uriarte, and M. Hansen (2010, 3). Deforestation driven by urban population growth and agricultural trade in the twenty-first century. *Nature Geoscience 3*, 178–181.

Destiartono, M. E. and D. Hartono (2022). Does rapid urbanization drive deforestation? evidence from southeast asia. *Economics Development Analysis Journal 11*(4), 442–453.

Dhital, Y. P. and Q. Tang (2015). Soil bioengineering application for flood hazard minimization in the foothills of siwaliks, nepal. *Ecological Engineering 74*, 458–462.

DLR (2016). Global urban footprint. https://www.dlr.de/eoc/en/desktopdefault.aspx/tabid-9628/16557_read-40454/.

Donaldson, D. and A. Storeygard (2016). The View from Above: Applications of Satellite Data in Economics. *Journal of Economic Perspectives 30*(4), 171–198.

Düben, C. and M. Krause (2021). Population, Light, and the Size Distribution of Cities. *Journal of Regional Science 61*(1), 189–211.

Ehrhardt-Martinez, K., E. M. Crenshaw, and J. C. Jenkins (2002, 3). Deforestation and the environmental kuznets curve: A cross-national investigation of intervening mechanisms. *Social Science Quarterly 83*, 226–243.

Ehrlich, D., M. Melchiorri, A. J. Florczyk, M. Pesaresi, T. Kemper, C. Corbane, S. Freire, M. Schiavina, and A. Siragusa (2018). Remote sensing derived built-up area and population density to quantify global exposure to five natural hazards over time. *Remote Sensing 10*(9), 1378.

Ehrlich, M. V., C. A. Hilber, and O. Schöni (2018). Institutional settings and urban sprawl: Evidence from europe. *Journal of Housing Economics 42*, 4–18. Housing in Europe: a different continent – a continent of differences.

ESA Land Cover CCI project team: Defourny, P. (2019). Global Land Cover Maps, Version 2.0.7.

European Environment Agency (2016, 6). Urban sprawl in europe - joint EEA-FOEN report. European Environment Agency. EEA Report No 11/2016.

Evans, G. and M. Pickup (2010). Reversing the Causal Arrow: The Political Conditioning of Economic Perceptions in the 2000–2004 U.S. Presidential Election Cycle. *The Journal of Politics 72*(4), 77–90.

Exavier, R. and P. Zeilhofer (2021). OpenLand: Quantitative Analysis and Visualization of LUCC. https://CRAN.R-project.org/package=OpenLand. R package version 1.0.2.

Fan, Y., J. Chen, G. Shirkey, R. John, S. Wu, H. Park, and C. Shao (2016). Applications of Structural Equation Modeling (SEM) in Ecological Studies: An Updated Review. *Ecological Processes 19*(5).

FAO (2015). GAUL 2015 Data License. Online. License Agreement.

Frenne, P. D., J. Lenoir, M. Luoto, B. R. Scheffers, F. Zellweger, J. Aalto, M. B. Ashcroft, D. M. Christiansen, G. Decocq, K. D. Pauw, S. Govaert, C. Greiser, E. Gril, A. Hampe, T. Jucker, D. H. Klinges, I. A. Koelemeijer, J. J. Lembrechts, R. Marrec, C. Meeussen, J. Ogée, V. Tyystjärvi, P. Vangansbeke, and K. Hylander (2021, 6). Forest microclimates and climate change: Importance, drivers and future research agenda. *Global Change Biology 27*, 2279–2297.

Glaeser, E. L. (2014). A world of cities: The causes and consequences of urbanization in poorer countries. *Journal of the European Economic Association 12*(5), 1154–1199.

Global High Resolution Population Denominators Project (2018). WorldPop. Online.

Gray, C. and V. Mueller (2012). Disasters and migration in Bangladesh. *Proceedings of the National Academy of Sciences 109*, 6000–6005.

Guha-Sapir, D., R. Below, and P. Hoyois (2009). EM-DAT: The CRED/OFDA International Disaster Database. http://www.emdat.be. Accessed: 13.09.2023.

Haile, G. G., Q. Tang, S. Sun, Z. Huang, X. Zhang, and X. Liu (2019, 6). Droughts in east africa: Causes, impacts and resilience. *Earth-Science Reviews 193*, 146–161.

Henningsen, A. and J. D. Hamann (2007). systemfit: A package for estimating systems of simultaneous equations in r. *Journal of Statistical Software 23*(4), 1–40.

Huang, C., R. Mcdonald, and K. Seto (2018). The Importance of Land Governance for Biodiversity Conservation in an Era of Global Urban Expansion, Landscape and Urban Planning. *Landscape and Urban Planning 173*, 44–50.

Jessoe, K., D. Manning, and J. Taylor (2018). Climate Change and Labour Allocation in Rural Mexico: Evidence from Annual Fluctuations in Weather. *The Economic Journal 182*, 230–261.

Joseph, G. and Q. Wodon (2013). Is Internal Migration in Yemen Driven by Climate or Other Socio-Economic Factors? *Review of International Economics 21*, 2032–2065.

Kaczan, D. and J. Orgill-Meyer (2020). The Impact of Climate Change on Migration: A synthesis of Recent Empirical Insights. *Climatic Change 158*, 281–300.

Kong, X., S. Ghaffar, M. Determann, K. Friese, S. Jomaa, C. Mi, T. Shatwell, K. Rinke, and M. Rode (2022, 8). Reservoir water quality deterioration due to deforestation emphasizes the indirect effects of global change. *Water Research 221*.

Koop, G. and L. Tole (1999, 2). Is there an environmental kuznets curve for deforestation? *Journal of Development Economics 58*, 231–244.

Li, X. and J. Xiao (2019). Mapping photosynthesis solely from solar-induced chlorophyll fluorescence: A global, fine-resolution dataset of gross primary production derived from oco-2. *Remote Sensing 11*(21).

Li, X., Y. Zhou, M. Zhao, and X. Zhao (2020, 6). A harmonized global nighttime light dataset 1992–2018. *Scientific Data 7*, 168.

Liebmann, B. and C. Smith (1996, June). Noaa interpolated outgoing longwave radiation (olr) 1991-2020. https://psl.noaa.gov/data/gridded/data.olrcdr.interp.html. Original Source: NOAA PSL.

Marchiori, L., J.-F. Maystadt, and I. Schumacher (2012). The Impact of Weather Anomalies on Migration in Sub-Saharan Africa. *Journal of Environmental Economics and Management 63*, 355–374.

MEA, M. E. A. (2005). *Ecosystems and Human Well-being: Biodiversity Synthesis*. Washington, DC: World Resources Institute.

Morice, C. P., J. J. Kennedy, N. A. Rayner, J. P. Winn, E. Hogan, R. E. Killick, R. J. H. Dunn, T. J. Osborn, P. D. Jones, and I. R. Simpson (2021). An updated assessment of near-surface temperature change from 1850: The hadcrut5 data set. *Journal of Geophysical Research: Atmospheres 126*(3), e2019JD032361. e2019JD032361 2019JD032361.

Nazareno, A. G. and W. F. Laurance (2015, 3). Brazil's drought: Beware deforestation. *Science 347*, 1054.

Ober, K. (2019). The Links Between Climate Change, Disasters, Migration and Social Resilience in Asia: A Literature Review. ADB Economics Working Paper no. 586, Asian Development Bank.

Panwar, V. and S. Sen (2020, 7). Disaster damage records of em-dat and desinventar: A systematic comparison. *Economics of Disasters and Climate Change 4*, 295–317.

Peri, G. and A. Sasahara (2019). Impact of Global Warming on Rural-Urban Migrations: Evidence from Global Big Data. NBER Working Paper no. 25728, National Bureau of Economic Research.

Scalenghe, R. and F. A. Marsan (2009). The anthropogenic sealing of soils in urban areas. *Landscape and Urban Planning 90*(1), 1–10.

Schmidt, P. (1990, 3). Three-stage least squares with different instruments for different equations. *Journal of Econometrics 43*, 389–394.

Smith, C., J. C. Baker, and D. V. Spracklen (2023, 3). Tropical deforestation causes large reductions in observed precipitation. *Nature 615*, 270–275.

Stocker, T. (2014). *Climate change 2013: the physical science basis: Working Group I contribution to the Fifth assessment report of the Intergovernmental Panel on Climate Change*. Cambridge university press.

Sundberg, R. and E. Melander (2013). Introducing the ucdp georeferenced event dataset. *Journal of Peace Research 50*(4).

Tembata, K., Y. Yamamoto, M. Yamamoto, and K. Matsumoto (2020, 8). Don't rely too much on trees: Evidence from flood mitigation in china. *Science of the Total Environment 732*.

Tobias, S., F. Conen, A. Duss, L. M. Wenzel, C. Buser, and C. Alewell (2018). Soil sealing and unsealing: State of the art and examples. *Land Degradation & Development 29*(6), 2015–2024.

UNISDR (n.d.). DesInventar Disaster Inventory System: Methodological Guide. Online. Version 10.1.2.

United Nations (2018). *World Urban Prospects, the 2018 Revision*. United Nations New York.

United Nations Development Programme (2024). Human Development Index. https://hdr.undp.org/data-center/human-development-index. Accessed: 2024-05-21.

van Dijk, A. I., M. van Noordwijk, I. R. Calder, S. L. Bruijnzeel, J. A. Schellekens, and N. A. Chappell (2009). Forest-flood relation still tenuous - comment on 'global evidence that deforestation amplifies flood risk and severity in the developing world'by c. j. a. bradshaw, n.s. sodi, k. s.-h. peh and b.w. brook. *Global Change Biology 15*, 110–115.

van Vliet, J. (2019). Direct and Indirect Loss of Natural Area from Urban Expansion. *Nature Sustainability 2*, 755–763.

Wang, P.-H., P. Minnis, B. A. Wielicki, T. Wong, and L. B. Vann (2002). Satellite observations of long-term changes in tropical cloud and outgoing longwave radiation from 1985 to 1998. *Geophysical Research Letters 29*(10), 37–1–37–4.

Wooldridge, J. M. (2012). *Introductory Econometrics: A Modern Approach* (5th ed.). New Delhi: Cengage Learning.

Xing, C. and J. Zhang (2017). The preference for larger cities in china: Evidence from rural-urban migrants. *China Economic Review 43*, 72–90.

Zhang, X., H. Wan, F. W. Zwiers, G. C. Hegerl, and S.-K. Min (2013). Attributing intensification of precipitation extremes to human influence. *Geophysical Research Letters 40*(19), 5252–5257.

# A Appendix: Data Summary

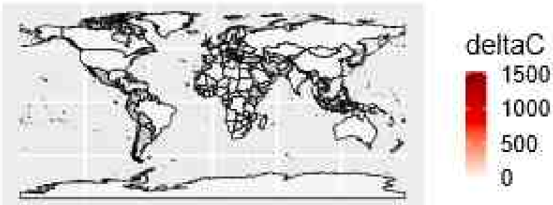


**(a)** Change in city size in $km^2$ aggregated between 2000 and 2013 (DesInventar)

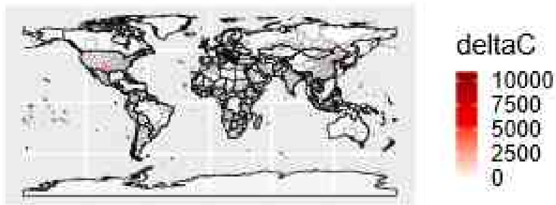


**(b)** Change in city size in $km^2$ aggregated between 2000 and 2018 (EM-DAT)

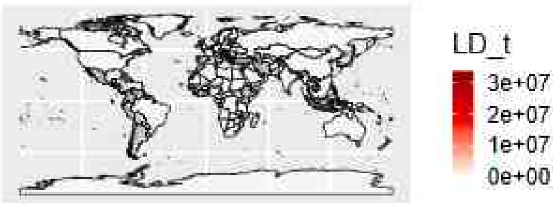


**(c)** Economic drought damages in US $ aggregated between 2000 and 2013 (DesInventar)

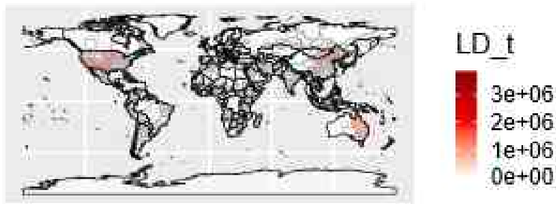


**(d)** Economic drought damages in US $ aggregated between 2000 and 2018 (EM-DAT)

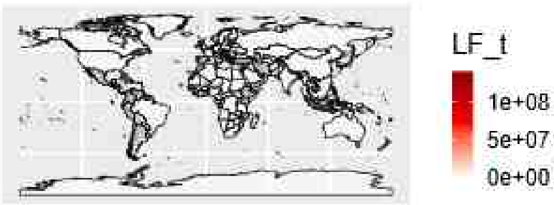


**(e)** Economic flood damages in US $ aggregated between 2000 and 2013 (DesInventar)


**(f)** Economic flood damages in US $ aggregated between 2000 and 2018 (EM-DAT)

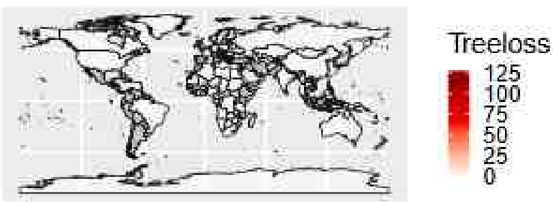


**(g)** Tree cover loss with subsequent sealed or bare land-cover in $km^2$ aggregated between 2000 and 2013 (DesInventar)


**(h)** Tree cover loss with subsequent sealed or bare land-cover in $km^2$ aggregated between between 2000 and 2018 (EM-DAT)

**Figure A-1** – Spatial distribution of variables of interest

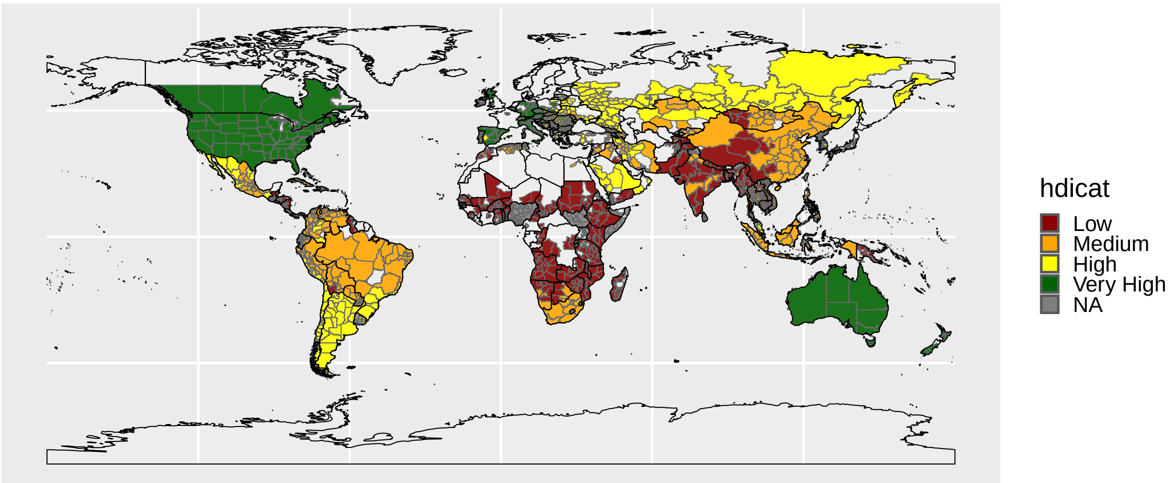


**Figure A-2** – Initial Human Development Index category of included NUTS-1 regions in 2001.

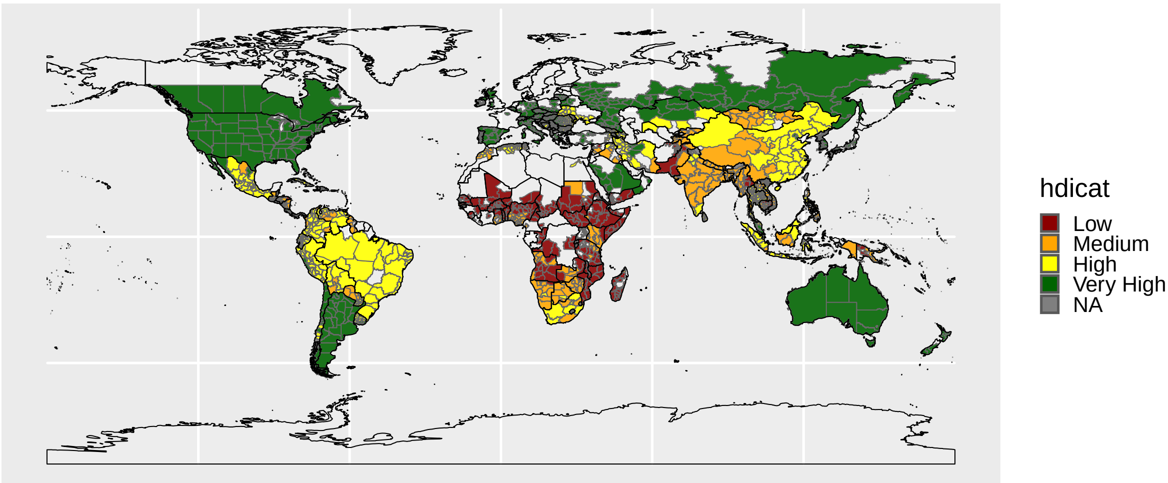


**Figure A-3** – Initial Human Development Index category of included NUTS-1 regions in 2018.

**Table A-1** – Included variables

| Variable | Description | Source |
|---|---|---|
| $C_t$ | city area/size | ESA Land Cover CCI project team: Defourny (2019) |
| $TSB_t$ | Treecover loss with subsequent surface sealing or bare area | ESA Land Cover CCI project team: Defourny (2019) |
| $LF_t$ | Economic losses from floods | UNISDR (nd), Guha-Sapir et al. (2009) |
| $LD_t$ | Economic losses from droughts | UNISDR (nd), Guha-Sapir et al. (2009) |
| $P_{U,t}$ | population count (urban) | Global High Resolution Population Denominators Project (2018) |
| $P_{nU,t}$ | population count (non-urban) | Global High Resolution Population Denominators Project (2018) |
| $NTL_{nU,t}$ | mean NTL (non-urban) | Bluhm and Krause (2022), Li et al. (2020) |
| $NTL_{U,t}$ | mean NTL (urban) | Bluhm and Krause (2022), Li et al. (2020) |
| $F_t$ | Number of floods | UNISDR (nd), Guha-Sapir et al. (2009) |
| $D_t$ | Number of droughts | UNISDR (nd), Guha-Sapir et al. (2009) |
| $Ft_{C,t}$ | Fatalities from violent conflicts | Sundberg and Melander (2013), Davies et al. (2023) |
| $T_t$ | Tree cover | ESA Land Cover CCI project team: Defourny (2019) |
| $S_t$ | Shrub cover | ESA Land Cover CCI project team: Defourny (2019) |
| $V_t$ | Other vegetation | ESA Land Cover CCI project team: Defourny (2019) |
| $B_t$ | Bare ground | ESA Land Cover CCI project team: Defourny (2019) |
| $Cr_t$ | Crop cover | ESA Land Cover CCI project team: Defourny (2019) |

# B Appendix: Land cover and land cover change variables

To calculate land cover changes while considering consecutive land cover, we utilized the annual land cover satellite products by ESA Land Cover CCI project team: Defourny (2019) spanning from the year 1999 to 2020. We applied the *OpenLand* R package Exavier and Zeilhofer (2021) to compute the area of land cover changes for each class, as classified in the first column of Table B-1. The resulting contingency table encompasses land cover transitions for all input rasters of a time series and the area of a specific land cover class that remains unchanged between two consecutive years.

Next, we implemented a two-stage aggregation process for land cover change variables, as well as for stock variables (the area within each class that was unaffected between two years). This two-stage aggregation enables us to conduct tests for heterogeneous effects with regard to tree cover as a robustness check. This is based on the different ecosystem services provided by broadleaved and needle-leaved forest ecosystems. Table B-1 illustrates the initial stage of this aggregation procedure. In the second step, we aggregated a tree cover stock variable from the new classes: Broadleaved, Needle, Mixed, and Unspecified. Subsequently, we constructed a tree cover loss variable from the instances where land cover transition occurred from the defined tree cover classes to either bare or sealed categories. Our analysis specifically emphasizes transitions to 'sealed' and 'bare' land cover classes to account for quasi-irreversible land changes—excluding potential regrowth—and recognizing that surface sealing is often preceded by a 'bare' land phase, indicating a non-reversible transition to urbanization or infrastructure development.

**Table B-1** – Aggregated Land Cover Classes based on ESA Land Cover CCI project team: Defourny (2019)

| Value | Label | Aggregated Class |
|---|---|---|
| 10 | Cropland rainfed | Crop |
| 11 | Herbaceous cover | Other vegetation |
| 12 | Tree or shrub cover | Unspecified |
| 20 | Cropland irrigated or post-flooding | Crop |
| 30 | Mosaic cropland (>50%) / natural vegetation | Crop |
| 40 | Mosaic natural vegetation / cropland (<50%) | Crop |
| 50 | Tree cover broadleaved evergreen closed to open | Broadleaved |
| 60 | Tree cover broadleaved deciduous closed to open | Broadleaved |
| 61 | Tree cover broadleaved deciduous closed | Broadleaved |
| 62 | Tree cover broadleaved deciduous open | Broadleaved |
| 70 | Tree cover needleleaved evergreen closed to open | Needle |
| 71 | Tree cover needleleaved evergreen closed | Needle |
| 72 | Tree cover needleleaved evergreen open | Needle |
| 80 | Tree cover needleleaved deciduous closed to open | Needle |
| 81 | Tree cover needleleaved deciduous closed | Needle |
| 82 | Tree cover needleleaved deciduous open | Needle |
| 90 | Tree cover mixed leaf type | Mixed |
| 100 | Mosaic tree and shrub / herbaceous cover | Unspecified |
| 110 | Mosaic herbaceous cover / tree and shrub | Other vegetation |
| 120 | Shrubland | Shrub |
| 121 | Evergreen shrubland | Shrub |
| 122 | Deciduous shrubland | Shrub |
| 130 | Grassland | Other vegetation |
| 140 | Lichens and mosses | Other vegetation |
| 150 | Sparse vegetation | Other vegetation |
| 151 | Sparse tree | Unspecified |
| 152 | Sparse shrub | Shrub |
| 153 | Sparse herbaceous cover | Other vegetation |
| 160 | Tree cover flooded fresh or brakish water | Unspecified |
| 170 | Tree cover flooded saline water | Unspecified |
| 180 | Shrub or herbaceous cover flooded | Other vegetation |
| 190 | Urban areas | Sealed |
| 200 | Bare areas | Bare |
| 201 | Consolidated bare areas | Bare |
| 202 | Unconsolidated bare areas | Bare |

# C Appendix: Hypothesized effects

| Variable | Hypothesis | Reference | Interpretation |
|---|---|---|---|
| | | Dependent variable: $\Delta C$ | |
| $LF_t$ | + | Hypothesis 1 | Economic losses from floods are a driver of urbanization |
| $LD_t$ | + | Hypothesis 1 | Economic losses from droughts as a driver of urbanization |
| $Ft_{C,t}$ | + | Camargo et al. (2020) | Armed conflicts force the rural population to migrate to safer urban areas. |
| $TSB_t$ | + | Adams and Adger (2013) | Environmental factors affect migration decisions through their impact on 'place utility', a concept encompassing both emotional and practical ties to a location. |
| $NTL_{U,t}$ | + | Düben and Krause (2021) | City growth goes in line with increasing economic activity as proxied for by lights. |
| $P_{nU,t}$ | + | D. da Mata et al. (2007) | Rural population supply potential |
| $P_{U,t}$ | + | Xing and Zhang (2017) Baum-Snow and Pavan (2011) | Larger urban areas have a stronger pull factor, e.g. due to wage premia and more amenities. |
| $NTL_{nU,t}$ | - | D. da Mata et al. (2007) | Increases of rural income opportunities reduce the "rural push" to urban areas. |

**Table C-1** – Hypothesized effects of variables in Equation (1)

| Variable | Hypothesis | Reference | Interpretation |
|---|---|---|---|
| | | Dependent variable: $TSB_t$ | |
| $\Delta C$ | + | Hypothesis 2 | Change in city area as a driver of tree cover loss |
| $T_t$, $S_t$, $V_t$, $B_t$, *sealed* | -/+ | | Stock variables controlling for the variablity in land cover. |
| $P_{nU,t}$ | + | Ehrhardt-Martinez et al. (2002) Destiartono and Hartono (2022) | Non-urban population drive tree cover loss through land take for agriculture |
| $NTL_{nU,t}$ | - | Destiartono and Hartono (2022) | Higher economic development is associated with lower rates of deforestation |
| $C_t$ | + | see Section 2.2 | More agriculture-reliant countries have higher rates of tree cover loss |
| $P_{U,t}$ | | DeFries et al. (2010) | The demand for agricultural products from an increasing urban population is a driver of tree loss |
| $NTL_{U,t}$ | +/- | Destiartono and Hartono (2022) Behnisch et al. (2022) | Higher economic development is associated with lower rates of deforestation but also higher rates of urban expansion |
| $Ft_{C,t}$ | -/+ | Christiansen et al. (2022) | Violent conflict can both increase and reduce tree loss |

**Table C-2** – Hypothesized effects of variables in Equation (2)

| Variable | Hypothesis | Reference | Interpretation |
|---|---|---|---|
| | | Dependent variable: $LD_t$ | |
| TSB_t | + | Hypothesis 3 | Tree cover loss increases drought damages |
| $T_t$, $S_t$, $V_t$ | -/+ | | Stock variables representing different classes of vegetation and their regulatory abilities and water needs, acknowledging the nonlinear and threshold-dependent nature of ecosystem services |
| $B_t$ | | | |
| $Cr_t$ | + | | Area of crops that are potentially exposed to droughts |
| $D_t$ | + | | An increased frequency of droughts increases the probability of damages. |
| $P_{U,t}$,$P_{nU,t}$ | +/- | | The larger the population, the more people are potentially affected by droughts but the better the adaptation potential might be. |
| $NTL_{U,t}$, $NTL_{nU,t}$ | - | | Higher economic development enables better adaptation to droughts and lower dependence on agricultural production. |

**Table C-3** – Hypothesized effects of variables in Equation (3)

| Variable | Hypothesis | Reference | Interpretation |
|---|---|---|---|
| | | Dependent variable: $LF_t$ | |
| TSB_t | + | Hypothesis 3 | Tree cover loss increases flood damages |
| $T_t$, $S_t$, $V_t$ | - | Frenne et al. (2021) Dhital and Tang (2015) | Stock variables representing different classes of vegetation and their regulatory abilities, acknowledging the nonlinear and threshold-dependent nature of ecosystem services |
| $B_t$ | + | Dhital and Tang (2015) | The fraction of bare ground vs. vegetated soil increases flood hazard. |
| $Cr_t$ | + | | Area of crops that are potentially exposed to floods |
| $F_t$ | +/- | | An increased frequency of floods increases the probability of damages but might also increase adaptation potential. |
| $P_{U,t}$,$P_{nU,t}$ | +/- | | The larger the population, the more people are potentially exposed to a flood, on the other hand a higher population correlates with better infrastructure, warnings systems and flood management. |
| $NTL_{U,t}$, $NTL_{nU,t}$ | +/- | | Higher economic development might correlate with better flood management and protective infrastructure but also higher values at risk. |

**Table C-4** – Hypothesized effects of variables in Equation (4)

# D Appendix: Further results and Robustness checks

**Table D-1** – Testing instrument strength for the global average results using the EM-DAT data base using an F-test. A significant test indicates sufficient instrument strength. The Wu-Hausmann test is used to assess the exogeneity of the instrumental variables. It compares the estimates from the IV regression model with those from an OLS regression. A significant result suggests endogeneity in the model, indicating that the IV approach is preferable to OLS. Since our model treats all tested variables as endogenous, we include the tested instruments in our analysis, even when the Wu-Hausman test suggests the results are not statistically significant.

| | df1 | df2 | statistic | p-value | Insr |
|---:|---:|---:|---:|---:|---|
| Weak instruments (LD_t) | 3.00 | 36929.00 | 1471.24 | 0.00 | cropdrought |
| Weak instruments (LF_t) | 3.00 | 36929.00 | 27.79 | 0.00 | AnnualAvgOLR |
| Weak instruments (Treeloss_no_veg) | 3.00 | 36929.00 | 2157.53 | 0.00 | T2SH_lag9 |
| Wu-Hausman | 3.00 | 36926.00 | 6.50 | 0.00 | |
| Weak instruments | 1.00 | 36927.00 | 2186.48 | 0.00 | needle_lag9 |
| Wu-Hausman1 | 1.00 | 36926.00 | 3.73 | 0.05 | |
| Weak instruments1 | 1.00 | 36927.00 | 2187.08 | 0.00 | needle_lag9 |
| Wu-Hausman2 | 1.00 | 36926.00 | 0.00 | 0.97 | |
| Weak instruments2 | 1.00 | 36925.00 | 140.33 | 0.00 | C2S_lag9 |
| Wu-Hausman3 | 1.00 | 36924.00 | 8.44 | 0.00 | |

**Table D-2** – Testing instrument strength for the global average results using the Desinventar data base using an F-test. A significant test indicates sufficient instrument strength. The Wu-Hausmann test is used to assess the exogeneity of the instrumental variables. It compares the estimates from the IV regression model with those from an OLS regression. A significant result suggests endogeneity in the model, indicating that the IV approach is preferable to OLS. Since our model treats all tested variables as endogenous, we include the tested instruments in our analysis, even when the Wu-Hausman test suggests the results are not statistically significant.

| | df1 | df2 | statistic | p-value | Insr |
|---:|---:|---:|---:|---:|---|
| Weak instruments (LD_t) | 3.00 | 14360.00 | 80.18 | 0.00 | mixed_lag9 |
| Weak instruments (LF_t) | 3.00 | 14360.00 | 32.68 | 0.00 | cropflood |
| Weak instruments (Treeloss_no_veg) | 3.00 | 14360.00 | 443.31 | 0.00 | T2C_lag9 |
| Wu-Hausman | 3.00 | 14357.00 | 16.21 | 0.00 | |
| Weak instruments | 1.00 | 14358.00 | 1291.37 | 0.00 | T2C_lag9 |
| Wu-Hausman1 | 1.00 | 14357.00 | 0.00 | 0.94 | |
| Weak instruments1 | 1.00 | 14358.00 | 1290.86 | 0.00 | T2C_lag9 |
| Wu-Hausman2 | 1.00 | 14357.00 | 0.15 | 0.70 | |
| Weak instruments2 | 1.00 | 14356.00 | 28.02 | 0.00 | C2S_lag9 |
| Wu-Hausman3 | 1.00 | 14355.00 | 2.40 | 0.12 | |

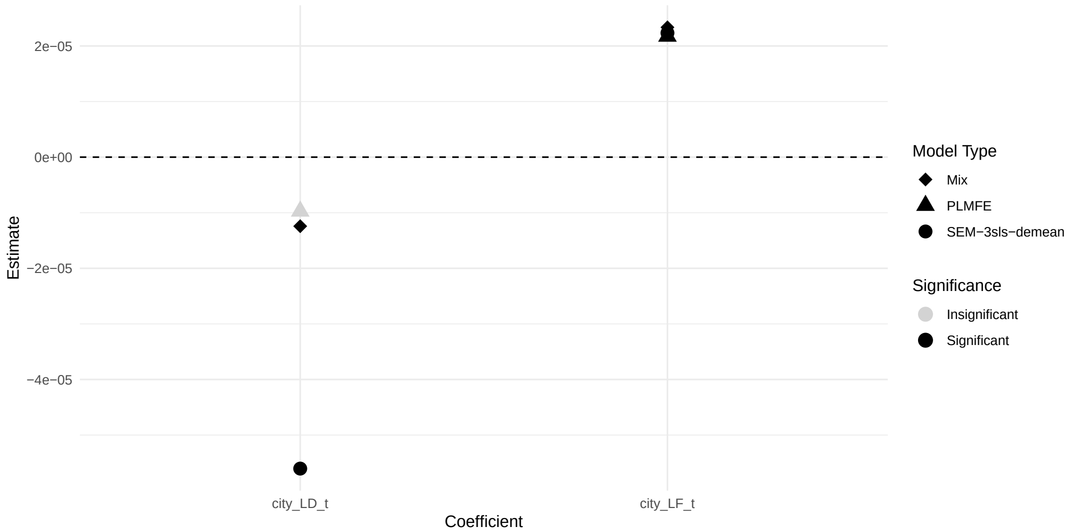


**(a)** $\Delta C \leftarrow LD_t$ and $\Delta C \leftarrow LF_t$ (H1)

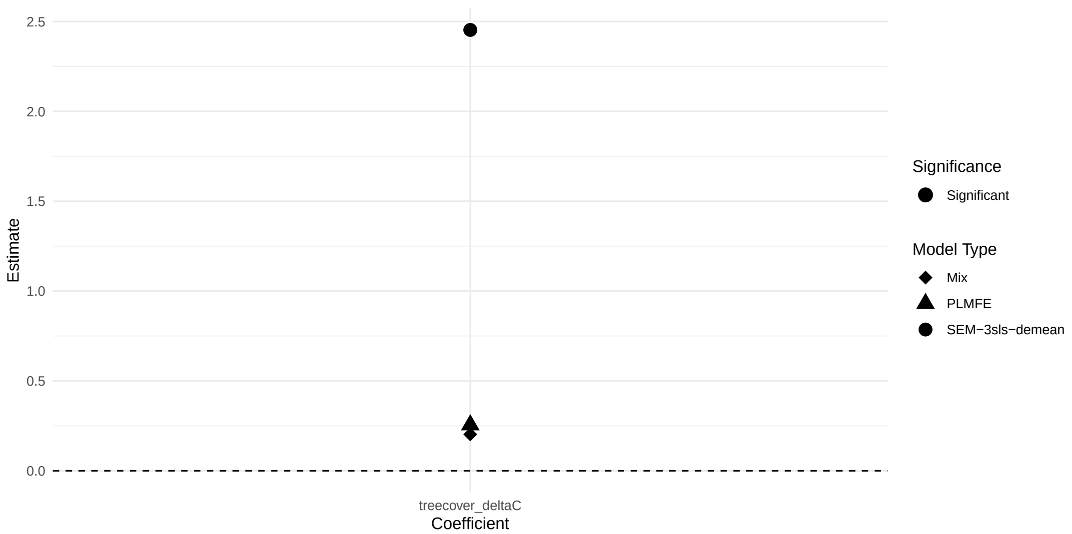


**(b)** $TSB_t \leftarrow \Delta C$ (H2)

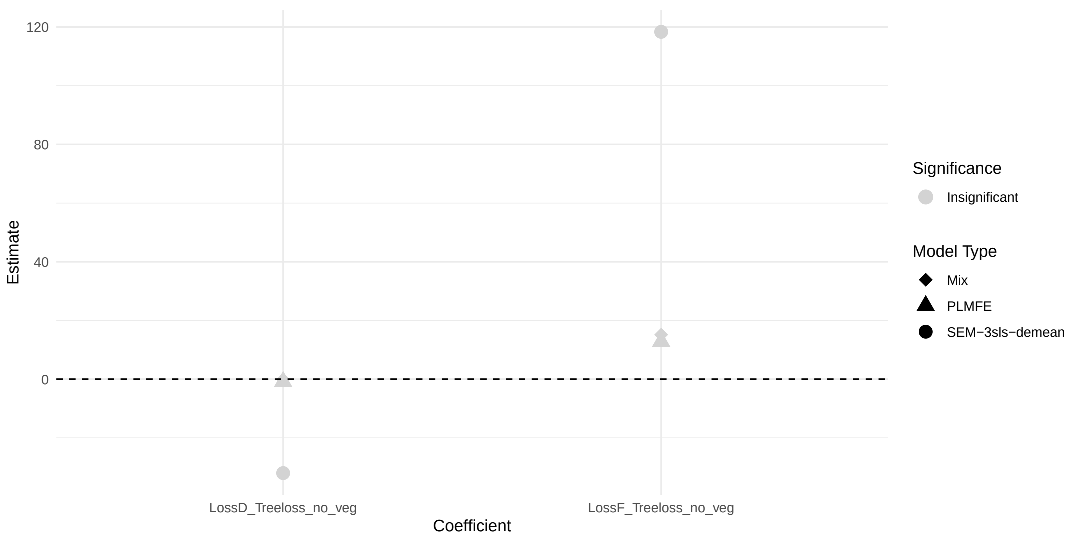


**(c)** $LD_t \leftarrow TSB_t$ and $LF_t \leftarrow TSB_t$ (H3)

**Figure D-1** – Robustness of results across estimation strategies for Europe using the EM-DAT data (N=8532).

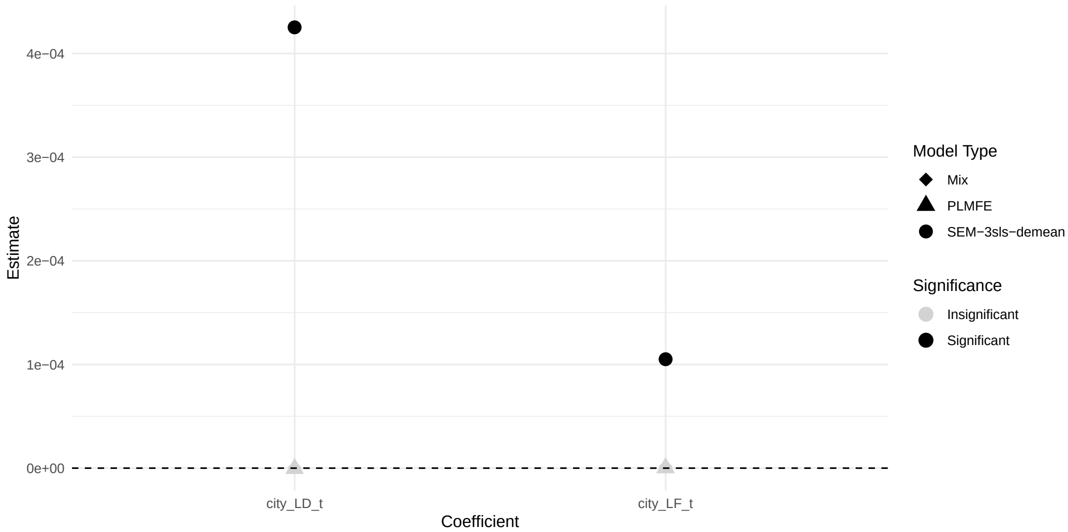


**(a)** $\Delta C \leftarrow LD_t$ and $\Delta C \leftarrow LF_t$ (H1)

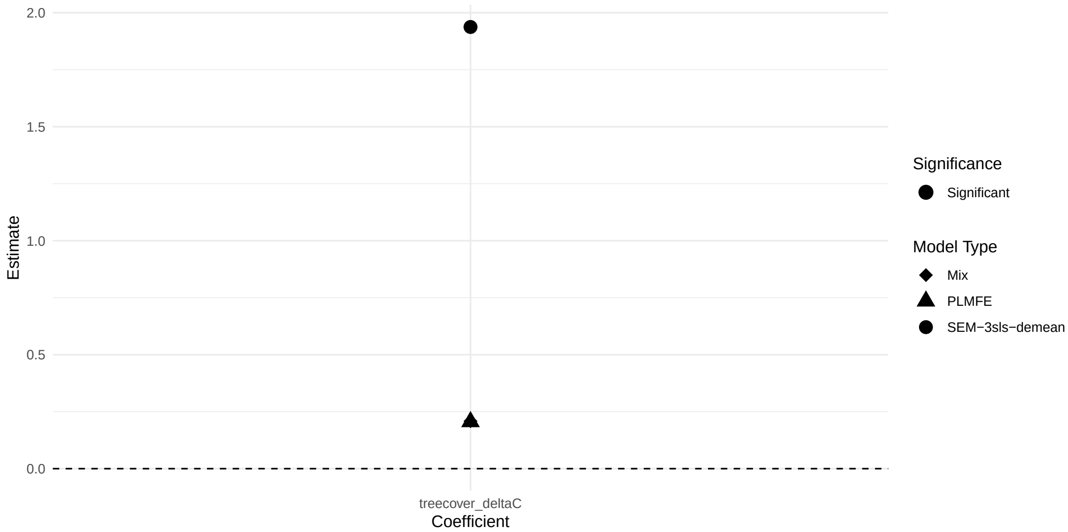


**(b)** $TSB_t \leftarrow \Delta C$ (H2)

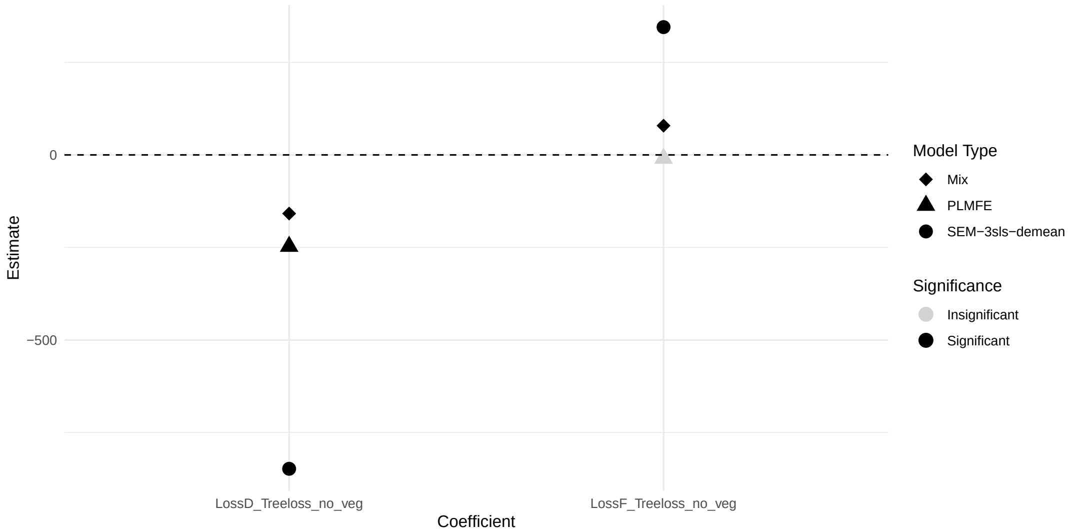


**(c)** $LD_t \leftarrow TSB_t$ and $LF_t \leftarrow TSB_t$ (H3)

**Figure D-2** – Robustness of results across estimation strategies for Africa using the EM-DAT data (N=9651).

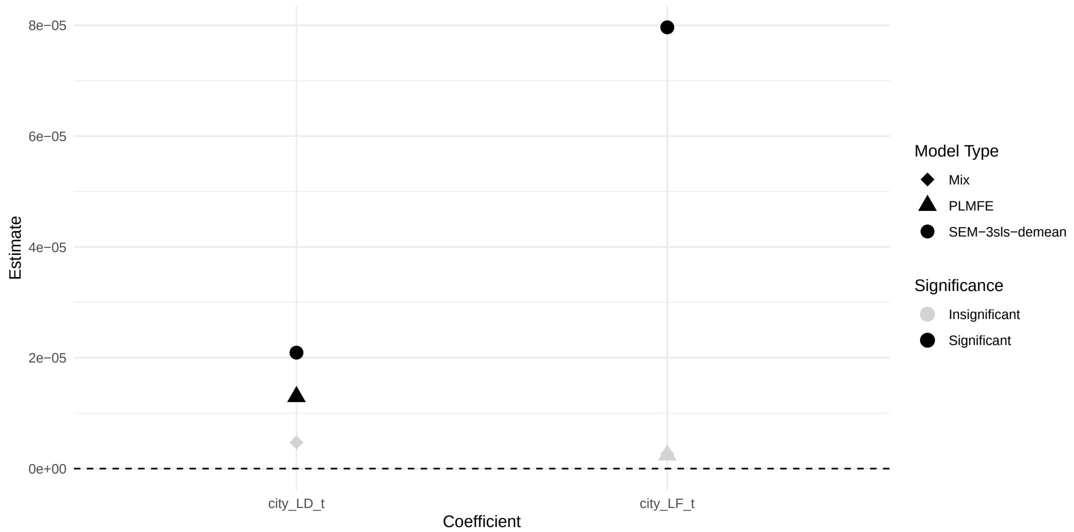


**(a)** $\Delta C \leftarrow LD_t$ and $\Delta C \leftarrow LF_t$ (H1)

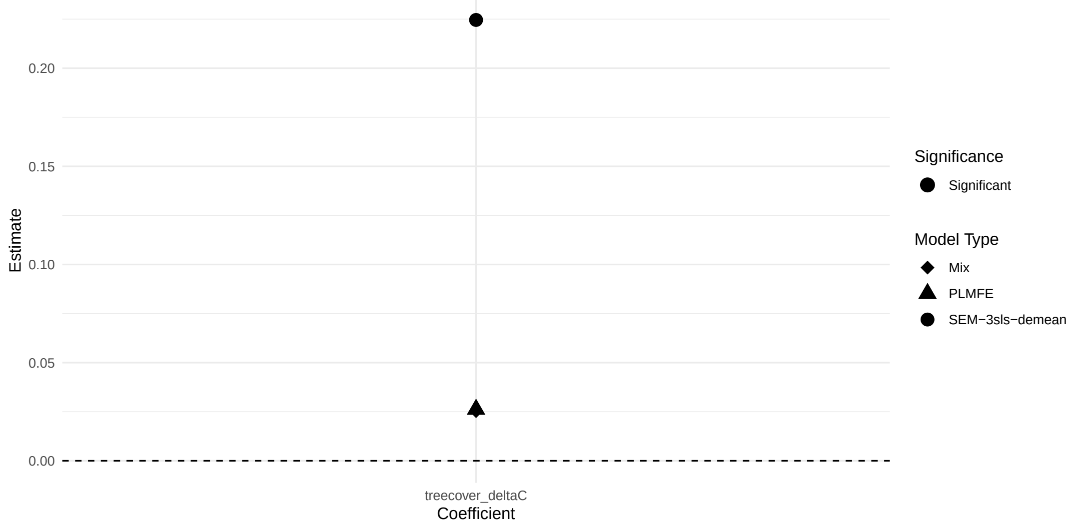


**(b)** $TSB_t \leftarrow \Delta C$ (H2)

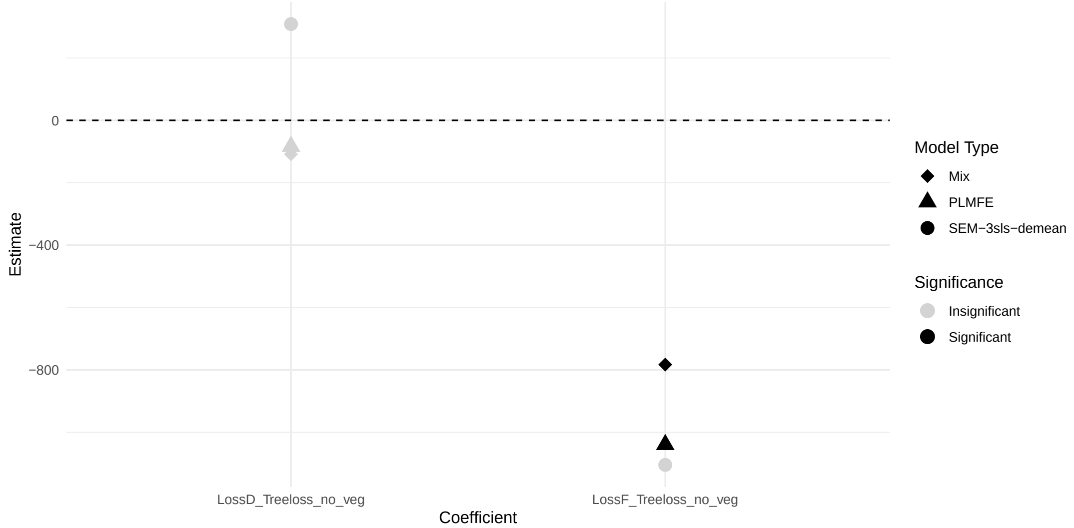


**(c)** $LD_t \leftarrow TSB_t$ and $LF_t \leftarrow TSB_t$ (H3)

**Figure D-3** – Robustness of results across estimation strategies for Asia using the EM-DAT data (N=11364).

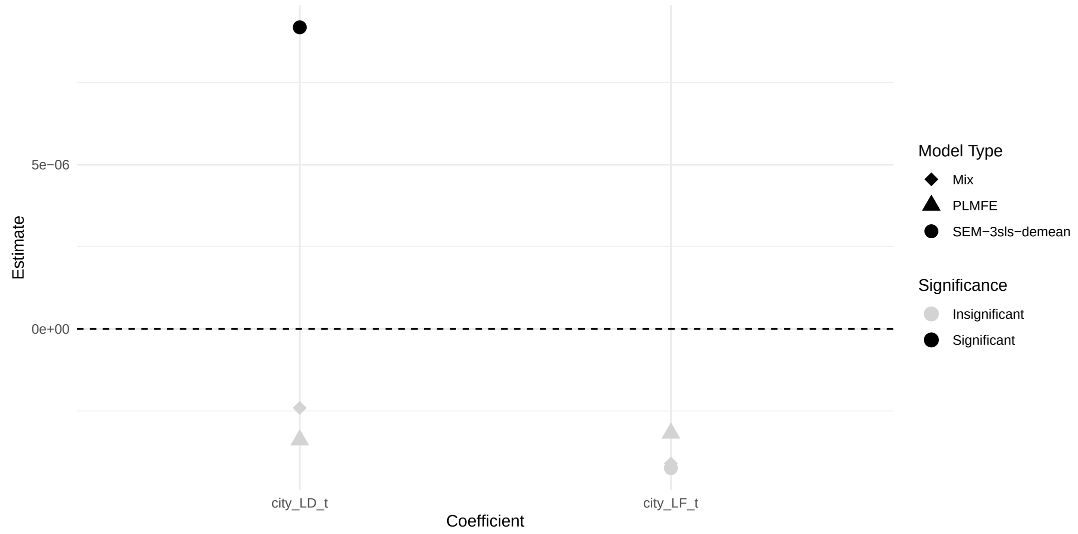


**(a)** $\Delta C \leftarrow LD_t$ and $\Delta C \leftarrow LF_t$ (H1)

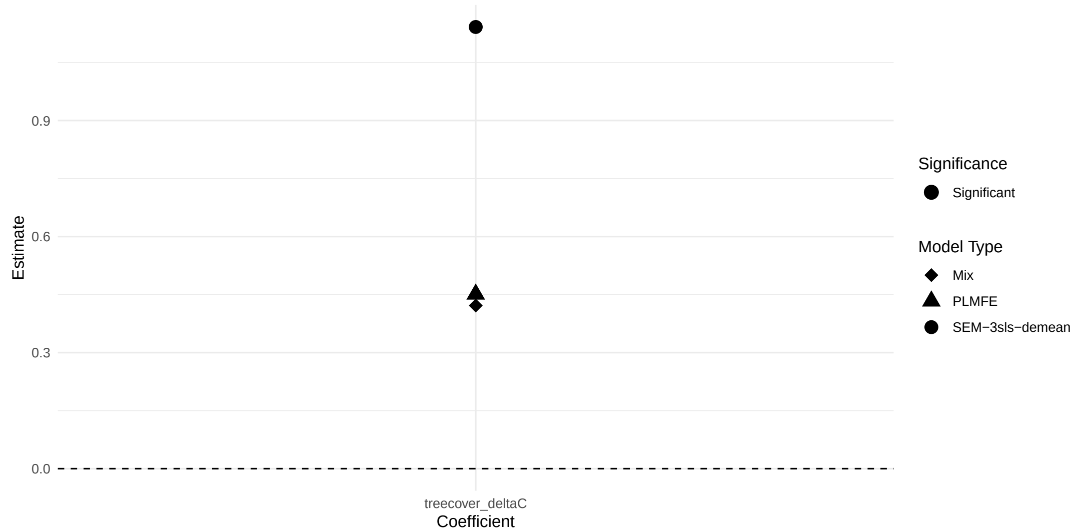


**(b)** $TSB_t \leftarrow \Delta C$ (H2)

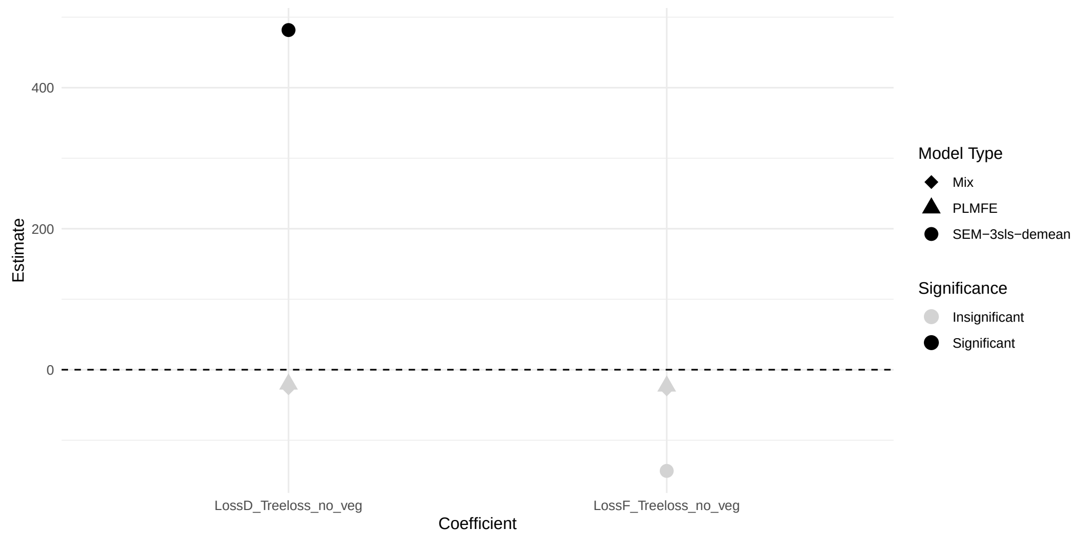


**(c)** $LD_t \leftarrow TSB_t$ and $LF_t \leftarrow TSB_t$ (H3)

**Figure D-4** – Robustness of results across estimation strategies for South America using the EM-DAT data (N=4394).

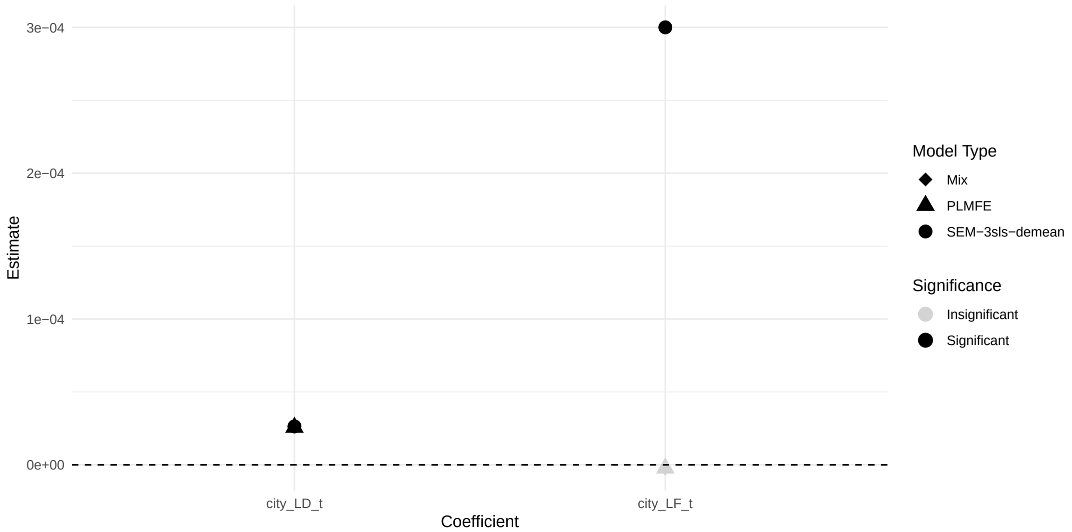


**(a)** $\Delta C \leftarrow LD_t$ and $\Delta C \leftarrow LF_t$ (H1)

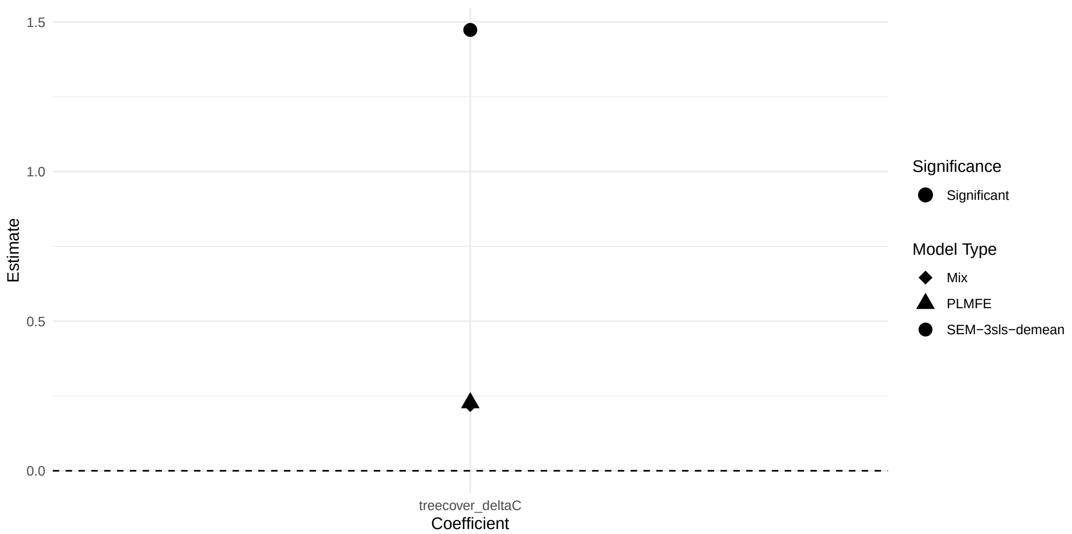


**(b)** $TSB_t \leftarrow \Delta C$ (H2)

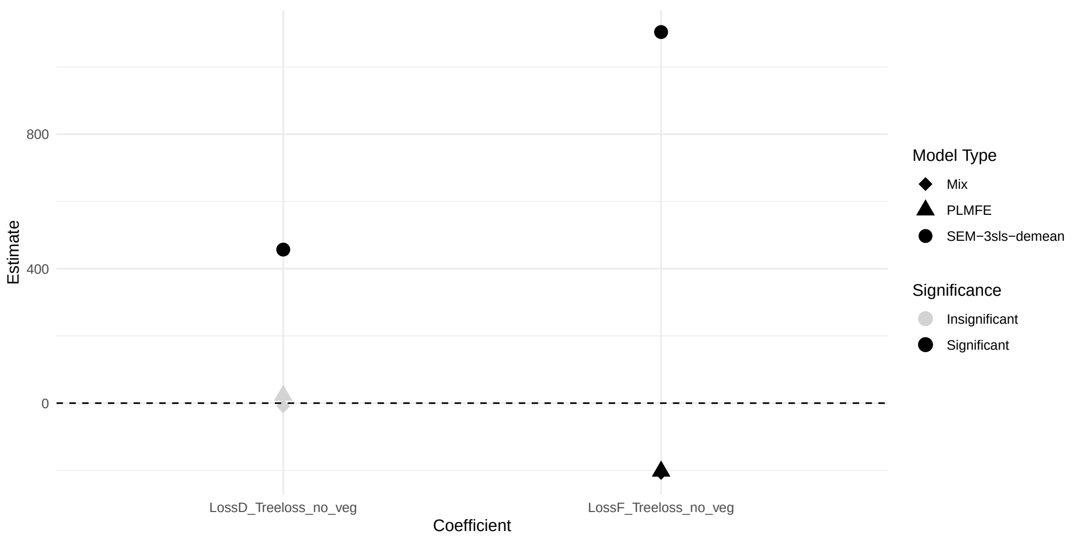


**(c)** $LD_t \leftarrow TSB_t$ and $LF_t \leftarrow TSB_t$ (H3)

**Figure D-5** – Robustness of results across estimation strategies for North America using the EM-DAT data (N=4327).

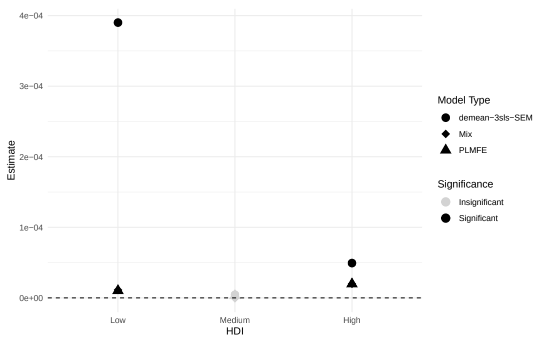


**(a)** $\Delta C \leftarrow LD_t$ (H1)

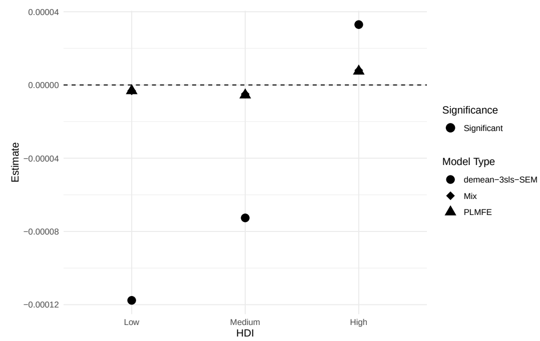


**(b)** $\Delta C \leftarrow LF_t$ (H1)

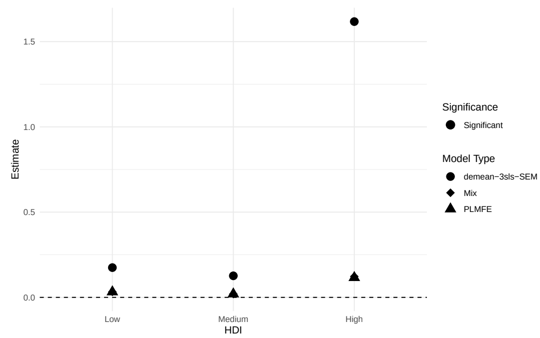


**(c)** $TSB_t \leftarrow \Delta C$ (H2)

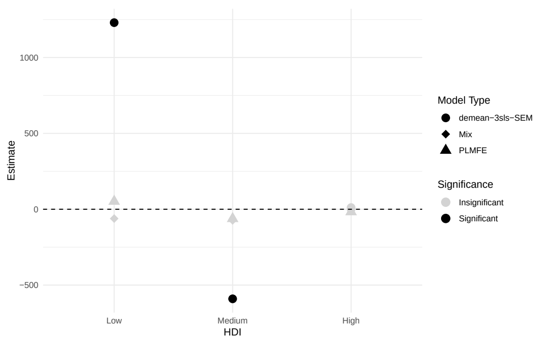


**(d)** $LD_t \leftarrow TSB_t$ (H3)

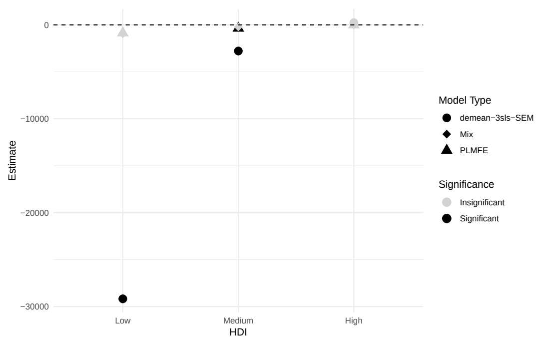


**(e)** $LF_t \leftarrow TSB_t$ (H3)

**Figure D-6** – Model effects by Human Development Index (HDI) category based on the EM-DAT data set estimated with a 3sls SEM, a panel and mixed effects model.

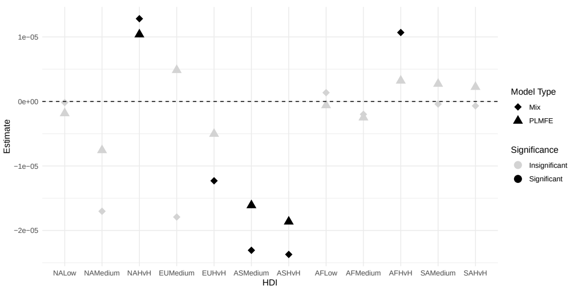


**(a)** $\Delta C \leftarrow LD_t$ (H1)

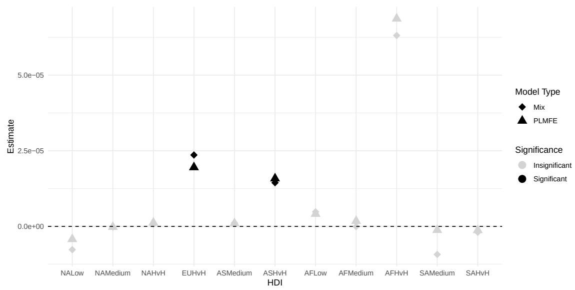


**(b)** $\Delta C \leftarrow LF_t$ (H1)

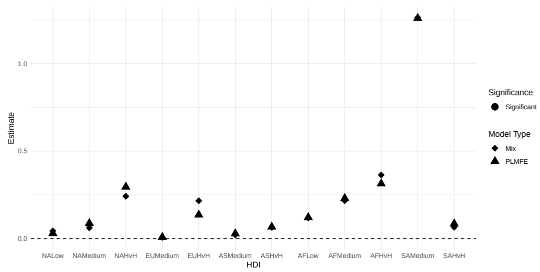


**(c)** $TSB_t \leftarrow \Delta C$ (H2)

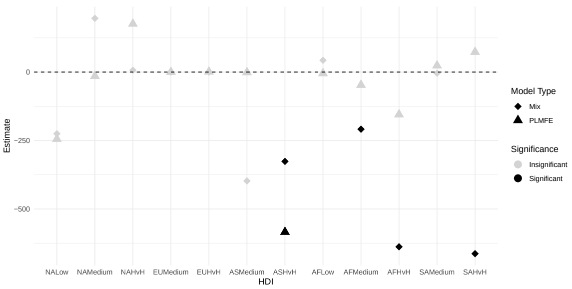


**(d)** $LD_t \leftarrow TSB_t$ (H3)

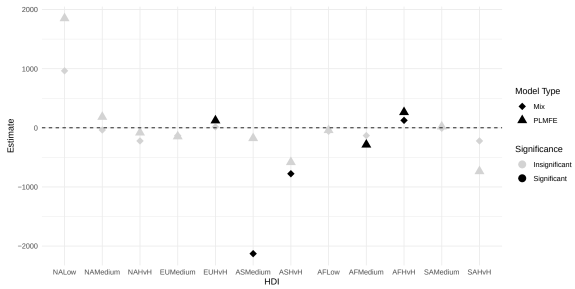


**(e)** $LF_t \leftarrow TSB_t$ (H3)

**Figure D-7** – Model effects by Human Development Index (HDI) and continent based on the EM-DAT data set estimated with a panel and mixed effects model. The instrumental variables necessary for SEM estimation are not sufficiently strong in this sub-categorization in all cases, thus we omit this estimation procedure win this sub-categorization of the data.